Scilight

Medical Materials Research

https://www.sciltp.com/journals/mmr

Review

Check for updates

Single-Atom Catalysts for Biomedical Applications: Enzyme-Like Activity, Precise Regulation, and Application Frontiers

Lijuan Kong [1,†], Yijie Wang [1,†], Lei Cao [1,2], Wenhao Li [1], Kun Zhang [1] and Wencheng Wu [1,*]

[1] Central Laboratory and Ultrasound Medicine and Computational Cardiology Key Laboratory of Sichuan Province, Sichuan Academy of Medical Sciences, Sichuan Provincial People's Hospital, University of Electronic Science and Technology of China, Chengdu 610072, China

[2] Department of Radiology, Sichuan Academy of Medical Sciences, Sichuan Provincial People's Hospital, University of Electronic Science and Technology of China, Chengdu 610072, China

* Correspondence: wuwencheng@uestc.edu.cn

† These authors contributed equally to this work.

How To Cite: Kong, L.; Wang, Y.; Cao, L.; et al. Single-Atom Catalysts for Biomedical Applications: Enzyme-Like Activity, Precise Regulation, and Application Frontiers. *Medical Materials Research* **2026**, *1*(1), 1. https://doi.org/10.53941/mmr.2026.100001

Received: 13 March 2026
Revised: 2 April 2026
Accepted: 3 April 2026
Published: 21 April 2026

Abstract: The discovery of nanoenzymes offers a novel approach to mimicking natural enzymes with both high stability and low cost. However, their complex surface structures and compositions often result in ambiguous catalytic sites and low atomic utilization. The emergence of single-atom catalysts (SACs) has overcome this bottleneck. By dispersing metal atoms in isolated form on a support, these catalysts achieve maximum atomic utilization and uniform coordination environments. This makes it possible for people to perfectly replicate the electrons and geometric structures of natural metallases on an atomic scale to construct SACs. These materials not only inherit the advantages of nanoenzymes, but also provide an ideal platform for clarifying the catalytic mechanism because of their clear and precisely controllable active sites. By regulating the central metal ion type, the type of coordinating atom and the carrier effect, its catalytic activity can be effectively optimized. Based on the enzyme-like activity of SACs and its activity regulation mechanism, this review explains the application of SACs in the field of biomedicine.

Keywords: single-atom catalysts; activity regulation; biomedical applications

1. Introduction

Natural enzymes play the role of high-efficiency catalysts in biological systems and have many core advantages, such as excellent catalytic efficiency and specificity [1,2]. However, as proteins, natural enzymes exhibit poor stability and are prone to inactivation by environmental factors like temperature and pH. Their production, purification, and storage incur high costs, and they are difficult to recover and reuse [3]. To overcome these limitations, scientists have dedicated efforts to finding alternatives.

As early as the 1970s, Michael E. Wilson et al. attempted to synthesize "artificial enzymes" by partially embedding rhodium(I) diphosphide into specific protein sites to construct asymmetric hydrogenation catalysts. These efforts opened a new and important branch of bionic chemistry [4,5]. In 2007, YAN et al. reported that magnetic nanoparticles Fe_3O_4 actually possess intrinsic enzyme-mimetic activity similar to natural peroxidase, capable of catalyzing the decomposition of hydrogen peroxide (H_2O_2) [6].This discovery opened an entirely new field. The term "nanozymes" was first coined by Scrimin, Pasquato, and colleagues to describe gold clusters protected by a thiol monolayer exhibiting outstanding ribonuclease activity [7]. Wang et al. extended this term to nanomaterials exhibiting enzymatic activity [8]. Subsequently, various nanozymes with activities mimicking oxidase, peroxidase and catalase were developed, such as CeO_2, carbon nanotubes, gold nanoclusters, and metal-

Copyright: © 2026 by the authors. This is an open access article under the terms and conditions of the Creative Commons Attribution (CC BY) license (https://creativecommons.org/licenses/by/4.0/).
Publisher's Note: Scilight stays neutral with regard to jurisdictional claims in published maps and institutional affiliations.

organic frameworks etc. [9–15]. Nanozymes have experienced rapid development and are widely applied in biosensing, disease diagnosis and treatment, environmental monitoring and remediation due to their high stability, low cost, scalability, and ease of modification [16–20].

Although nanozymes have achieved significant breakthroughs in stability and cost compared to natural enzymes, their catalytic performance still holds potential for further enhancement. The core catalytic site of traditional nanoenzymes is usually the metal atomic cluster on the surface of nanoparticles. These sites are unevenly distributed, and most of the atoms inside the particles cannot participate in the reaction. This leads to low atomic utilization rate, making it difficult for nanoenzymes to achieve the catalytic activity and selectivity of natural enzymes. In addition, the slow leakage of metal ions in the body may give potential toxicity to nanoenzymes [21–23]. In contrast, SACs anchor metal atoms in the form of single atoms on the carrier, avoiding the aggregation and embedding of nanoparticles, thus achieving higher atomic utilization and uniform active site structure. Their precise catalytic mechanism enables it to achieve high efficiency at lower doses, further enhancing biocompatibility, and their stable metal-carrier coordination bonds significantly reduce the leakage of metal ions, thus reducing the potential toxic risks [24,25].

Since the discovery of the first structurally defined SACs Pt_1/FeO_x by Qiao et al. in 2011, SACs have emerged as a frontier research hotspot [26]. Their applications have expanded from traditional thermal catalysis to cutting-edge fields such as electrocatalysis, photocatalysis, and biomedical catalysis, demonstrating immense potential. The development of SACs is briefly summarized in Figure 1 [27]. Previous reviews of SACs have primarily focused on different synthesis strategies or biomedical applications. This review centers on elucidating their biomedical applications by examining the catalytic mechanisms and regulatory mechanisms of catalytic activity in SACs.This paper first reviews enzyme-like activities and their regulation mechanisms in SACs. Building upon this foundation, it then discusses applications in tumor therapy, anti-inflammatory treatment, antimicrobial therapy, and biosensing. Finally, it explores the prospects and challenges for SACs in biomedical applications. This review aims to provide useful guidance for researchers in this field and further advance novel nanocatalytic antitumor strategies.

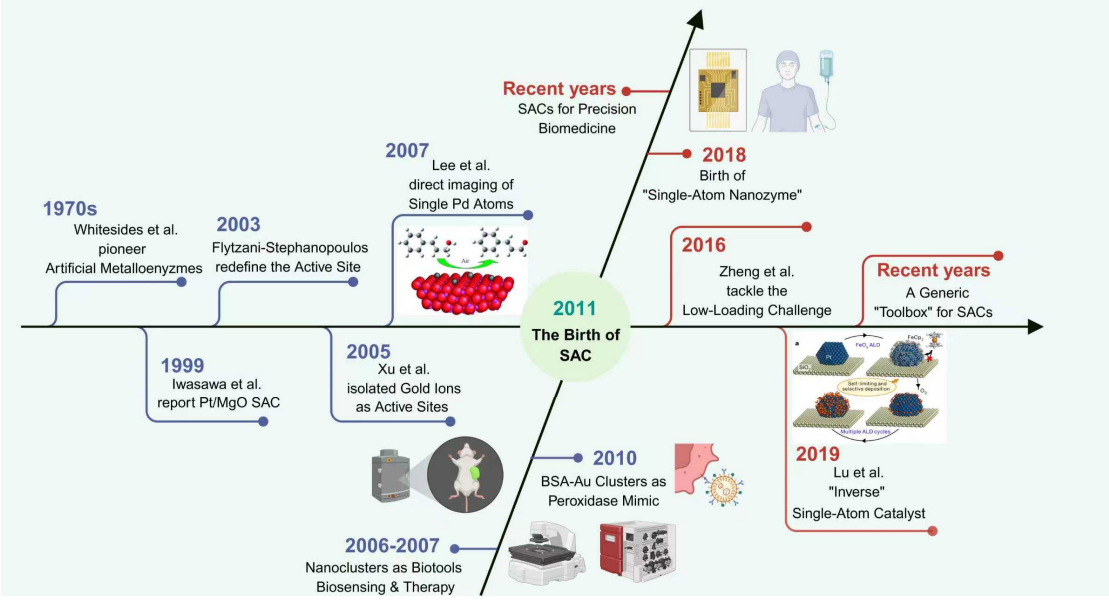

Figure 1. The development of SACs [5,28–33]. Copyright 2019, Springer Nature. Copyright 2007, John Wiley and Sons. Created with BioRender.com.

2. Catalytic Mechanisms and Activity Regulation of SACs

Traditional nanomaterial-catalyzed reactions typically occur on the catalyst surface or interface, engaging only a fraction of surface atoms. SACs achieve atomic-scale distribution of metals, with isolated active sites anchored via ionic interactions or covalent coordination with surrounding atoms. This confers multiple advantages: unsaturated metal atoms, unique electronic structures, maximum atomic utilization efficiency, and strong metal-support interactions. Similar to traditional nanoenzymes, SACs exhibit activities akin to oxidase (OXD), peroxidase (POD), and superoxide dismutase (SOD) (Figure 2). And by changing the metal center, carrier and coordination environment, its catalytic performance can be adjusted, and SACs for specific targets can be designed [34].

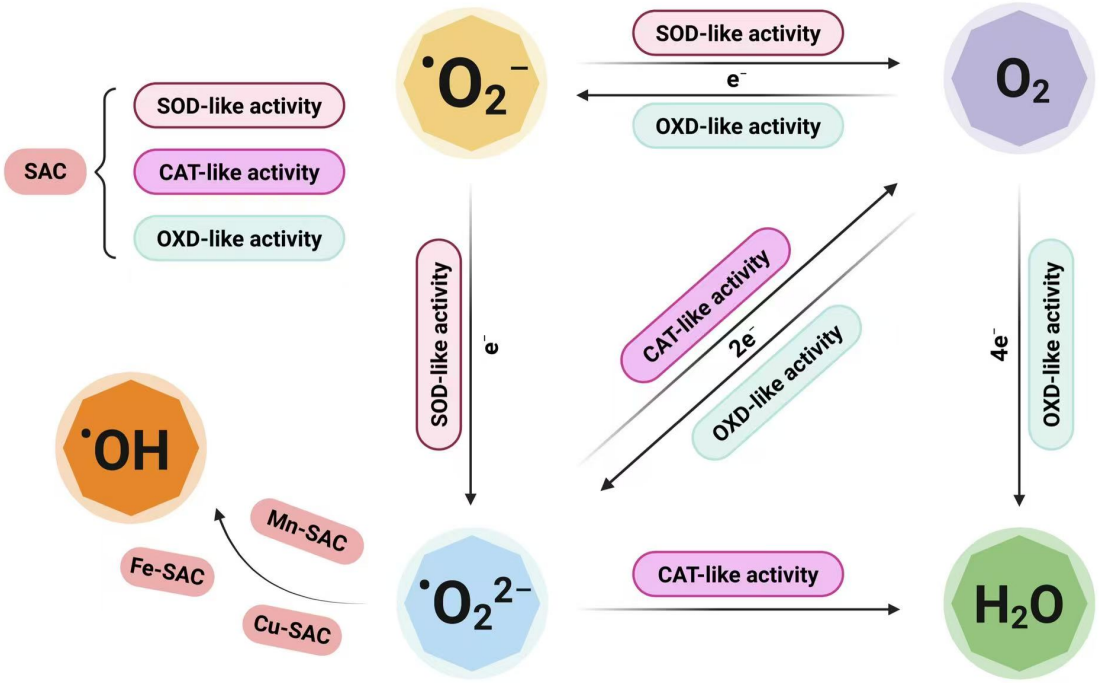

Figure 2. Common Enzyme-Like Activities and Reactive Oxygen Species Conversion in SACs. Created with BioRender.com.

2.1. Fenton-like Reactions and Fundamentals of Chemokinesis Therapy

The Fenton reaction is a classic catalytic oxidation process, in which ferrous ions (Fe^{2+}) catalyze the decomposition of H_2O_2 to produce hydroxyl radicals (·OH) with strong oxidation ability, thus efficiently degrading organic pollutants [35]. Fenton-like reaction refers to the use of other metal ions (copper, manganese, cobalt) or non-metallic catalysts to promote similar redox reactions, such as the peroxidase (POD) activity of nanoenzymes. Although the Fenton reaction has been widely used in the field of environmental restoration, its application in the biomedical field was initially limited by many restrictions, including harsh reaction conditions, low catalytic efficiency and poor biocompatibility, which hindered its comprehensive development [36–38]. With the progress of nanotechnology, more and more nanoenzymes with Fenton-like catalytic functions have been discovered. Using these nanomaterials to catalyze the overexpression of H_2O_2 in the tumor microenvironment under weakly acidic conditions, so as to generate ·OH in situ, which overcomes the key limitations of the traditional homogeneous Fenton reaction, such as strict pH dependence and low reaction efficiency. This mechanism forms the basis of chemodynamic therapy (CDT) and further enhances the therapeutic effect of CDT through a variety of strategies, including adjusting pH, consuming glutathione (GSH) and using it in combination with external energy sources (such as light and ultrasound) to achieve synergistic anti-cancer effect [39,40].

Nanoenzymes can not only enhance catalytic stability, but also achieve tumor targeting through surface functionalization, thus significantly improving treatment specificity and reducing systemic toxicity [41–44]. Similarly, SACs show excellent catalytic performance in Fenton-like reactions. Due to their unique properties, their effect is even significantly better than that of traditional nanoenzymes [45–48]. Qiao et al. developed a manganese-based SAC (Mn-N/C), which can efficiently catalyze the Fenton-like reaction of H_2O_2 decomposition into ·OH under acidic conditions. Compared with the traditional MnO_2, the catalyst not only shows better catalytic activity, but also induces the production of a large amount of reactive oxygen species (ROS) in tumor cells. Density functional theory (DFT) calculations show that during the reaction, H_2O_2 molecules are first adsorbed on the Mn-N_4 site with a lower energy barrier (0.16 eV). Subsequently, H_2O_2 isocleated to produce two ·OH species adsorbed in the center of manganese. Finally, an active ·OH species combines with adsorbed hydrogen to form an H_2O molecule, and desorbs under a lower energy barrier (0.64 eV) to complete the catalytic cycle. Another ·OH can be dissorted from the surface of the catalyst and diffused to the surrounding environment, thus inducing immunogenic cell death (ICD) and activating the cyclic GMP-AMP synthase (cGAS)-stimulator of interferon genes (STING)-type I interferon (IFN-I) signaling pathway, significantly enhancing the anti-tumor immune response of $CD8^+$ T cells. The study shows that Mn-N/C shows a synergistic anti-tumor effect when used in combination with anti-PD-

L1 antibodies, highlighting the broad application prospects of SACs in enhanced chemotherapy and combined immunotherapy. This research provides a crucial paradigm for designing highly efficient and specific SACs, while also showcasing their potential value in tumor immune regulation (Figure 3) [49].

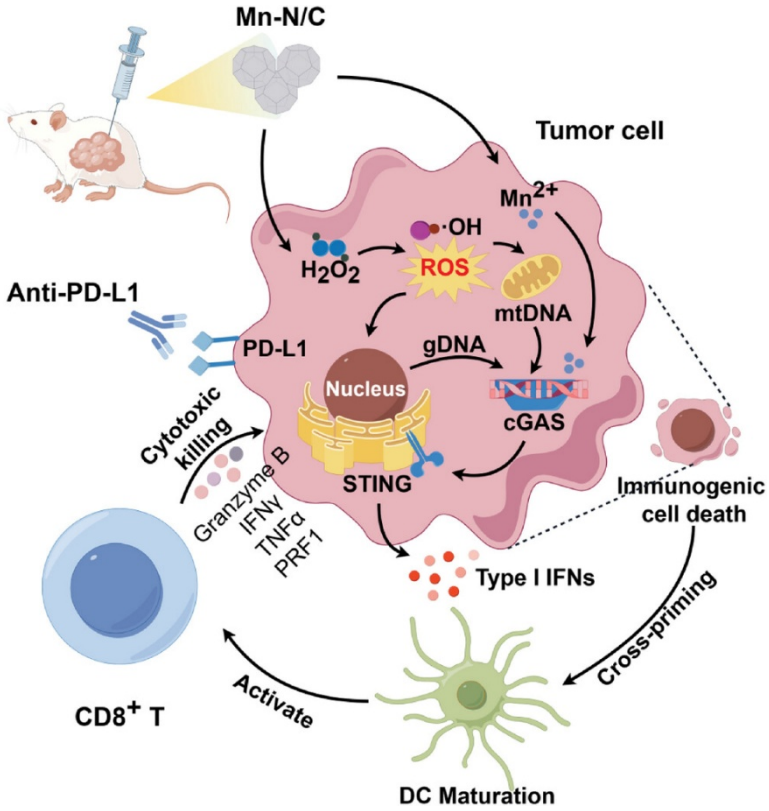

Figure 3. Schematic diagram of Mn-N/C for activating anti-tumor immune response. Conceptual and effective mechanisms of Mn-N/C in triggering immunogenic cell death and remodeling tumor immune microenvironment [49]. Copyright 2024, John Wiley and Sons.

Simultaneously, Fenton-like reactions can be combined with Sonodynamic therapy (SDT), radiotherapy (RT), and photothermal therapy (PTT)for disease treatment [50–52]. Feng et al. designed a spherical mesoporous Fe-N-C SACs for highly efficient antibacterial therapy. Beyond efficiently catalyzing low-concentration hydrogen peroxide (H_2O_2) to generate highly toxic hydroxyl radicals (·OH) for bacterial elimination, the Fe-N-C SAC's carbon framework structure endows it with exceptional photothermal properties, enabling rapid heat generation under near-infrared light irradiation. The photothermal effect synergizes with the catalytic process: locally elevated temperatures significantly enhance the nanozyme's catalytic activity, generating more radicals, while the heat itself physically damages bacteria. This "chemical catalysis + physical hyperthermia" synergistic strategy demonstrates vastly superior bactericidal and wound-healing capabilities in both in vitro and in vivo experiments compared to either method alone [53]. Chen et al. designed a novel FeMn-NC_e dual-atom SACs. By surface-modifying it with gold nanoparticles and loading STING agonist diamidobenzimidazole (diABZI) and programmed death-ligand 1 (PD-L1) aptamer, they constructed the multifunctional nanoplatform dAuFeMn-NC_e. This nanozyme exhibits outstanding peroxidase-mimetic activity in the tumor microenvironment, efficiently catalyzing hydrogen peroxide to generate hydroxyl radicals under X-ray irradiation. This induces DNA damage and activates the cGAS-STING immune pathway, reshaping the immunosuppressive tumor microenvironment and establishing long-term immune memory. Consequently, it effectively suppresses tumor growth and metastasis, achieving enhanced radiodynamic immunotherapy [54]. Therefore, combining the catalytic activity of SACs with other physical therapies can often achieve a synergistic effect, where "1+1>2". Furthermore, by precisely regulating the immune pathways related to a disease, the catalytic effect of SACs can be combined with related immune effects to achieve better therapeutic results [55,56].

2.2. Multifunctional Enzyme-Like Activity Spectrum

Beyond Fenton-like reactions dependent on peroxidase activity, SACs can mimic other enzymatic activities by regulating central metal types and coordination structures, enabling biomedical applications, such as oxidases,

antioxidases, and NADPH oxidases. The enzyme-like catalytic activity of SACs stems from their unique atomically dispersed active sites and tunable coordination microenvironments, enabling highly accurate mimicry of natural enzyme metal active pockets. Specifically, well-defined M-Nx sites (where M represents a metal atom and x is typically 4) achieve nearly 100% atomic utilization. Moreover, strong electron interactions between the support and metal center optimize the adsorption energy of reaction intermediates, significantly lowering the catalytic energy barrier [57,58]. For instance, Yan et al. constructed a carbon nanoframe-confined FeN_5 exhibiting catalytic behavior similar to that of the axial ligand-coordinated heme in cytochrome P450, with a reaction rate constant 70 times higher than that of commercial Pt/C [27]. The following sections will provide a detailed introduction to oxidase activity, antioxidant enzyme activity, and other enzyme activities such as NADPH enzyme.

2.2.1. Oxidase-Like Activities: Peroxidase (POD), Oxidase (OXD)

Fenton-like reactions occur under the catalysis of peroxidase (POD) activity, which is a metal-based SAC, converting H_2O_2 into ·OH with strong oxidizing power for the treatment of diseases [59]. Feng et al. doped single-atom iron (Fe) into graphitic-phase carbon nitride (C_3N_4) nanostructures nanocarrier, designing a unique chemically reactive Fe-C_3N_4 nanosheets (Fe-C_3N_4 NSs).

Under ultrasound irradiation, Fe single-atom doping enhances electron pair separation efficiency, enabling high-yield ROS generation for melanoma treatment. This reaction can be enhanced and synergistically combined with SDT to boost antitumor efficacy. The construction of Fe-C_3N_4 NSs provides an effective single-atom doping strategy for inorganic nanoscale photosensitizers to enhance ROS generation under ultrasonic stimulation, opening new avenues for semiconductor-based inorganic photosensitizers in tumor suppression applications [60].

Materials exhibiting oxidase-like activity can catalyze oxygen to generate ROS such as superoxide anions in vivo, enabling applications in bio-detection and disease therapy with broad potential in biomedicine [61–63]. Feng et al. successfully constructed Fe SACs, which Fe single atoms (FeSA) anchoring onto onion-like carbon (OLC) support (FeSA-OLC). This structure efficiently activates oxygen to generate ROS, exhibiting catalytic efficiency significantly superior to traditional nanoparticles and commercial platinum-carbon catalysts. Moreover, the material exhibits a photothermal enhancement effect for its enzyme-like activity: heat generated by near-infrared irradiation further accelerates ROS production, ultimately achieving efficient antibacterial activity through synergistic photothermal-catalytic effects [64]. SACs with oxidase-like activity can not only directly inhibit bacteria by catalyzing ROS but also achieve disease treatment by modulating metabolism [65]. Sun et al. constructed a sulfur-doped iron SAC, whose oxidase-like activity plays a dual core role: On one hand, it directly catalyzes ROS production; on the other, it synergizes with its bioorthogonal catalytic function to activate prodrugs in situ within tumor-associated macrophages. This jointly upregulates m^6A RNA methylation levels, thereby reprogramming pro-cancer M2 macrophages into anti-cancer M1 macrophages. Ultimately, it suppresses tumor growth and metastasis by activating immune responses [66].

SACs with OXD-like activity exhibit higher stability than natural oxidases, making them suitable for low-temperature disinfection and sterilization [67–69]. For addressing the global challenge of viral transmission in cold chain logistics, Qin et al. designed a FeN_4P_2 SAC that maintains high activity at −20 °C by fine-tuning the electronic structure through phosphorus atom doping at the Fe-N_4 center. By mimicking lipid oxidases, this catalyst directly catalyzes the peroxidation reaction of viral envelope lipids, targeting the conserved physical structure of viruses. It has achieved broad-spectrum low-temperature inactivation of a variety of coronaviruses and influenza viruses, overcoming the bottleneck of the failure of traditional chemical disinfectants at low temperatures. This breakthrough provides an innovative solution to block the cold chain transmission route, and also demonstrates the great potential of reasonably designed SAC in extreme environments [70]. The OXD-like activity of SACs often involves the generation of ROS through catalytic reactions, enabling applications in biomedical fields including sterilization, disinfection, and antitumor therapy [71].

2.2.2. Antioxidant Enzyme Activity: Catalase (CAT), Superoxide Dismutase (SOD), Glutathione Peroxidase (GPx)

Beyond oxidase-like activity, SACs can precisely mimic the functions of multiple antioxidant enzymes such as catalase, superoxide dismutase and so on. Their structural designability enables adaptation to diverse pH, temperature, and substrate environments, maintaining high stability even under physiological conditions. SACs are frequently employed in treating various diseases through the following four processes: (1) SOD catalyzes the conversion of superoxide anion into H_2O_2 and oxygen, (2) CAT catalyzes the conversion of H_2O_2 into oxygen and water, (3) GPx reduces H_2O_2 or toxic organic peroxides into harmless alcohols and water, (4)The accumulation of hydroxyl radicals in the body is also reduced due to oxygen production and H_2O_2 consumption during these catalytic processes [23,72–74]. Therefore, currently designed materials for scavenging ROS (ROS) often possess

all three enzymatic activities working synergistically to eliminate ROS in vivo, collectively contributing to disease diagnosis and treatment [75–78].

Li et al. developed a platinum-doped CeO_2 SAC (Pt/CeO_2) exhibiting multiple antioxidant enzyme activities including CAT, SOD, and GPx, with significantly higher catalytic efficiency than pure CeO_2.Research indicates this material not only efficiently scavenges ROS but also disrupts the α-glycerophosphate shuttle and malate-aspartate shuttle pathways by consuming H^+ around mitochondria. Following fusion of immune cells and tumor cells, increased expression of markers on the cell membrane surface facilitates nanoparticle-loaded shuttle pathways, inducing mitochondrial membrane potential depolarization and subsequently triggering mitochondrial autophagy eliminating dysfunctional mitochondria at their source and blocking sustained ROS production. To further enhance targeting and blood-brain barrier penetration, the research team encapsulated Pt/CeO_2 within activated neutrophil-like (HL-60) cell membrane (AHM) and modified it with rabies virus glycoprotein (RVG29), constructing the RVG29@AHM@Pt/CeO_2 nanomaterial system. In a Parkinson's disease model, this system specifically enriched in brain inflammatory regions and entered dopa mine neurons, achieving dual therapeutic effects: "treating symptoms" (clearing existing ROS) and "treating root causes" (inducing autophagy to clear dysfunctional mitochondria). This significantly improved both motor and non-motor symptoms in model mice. This research provides new materials and mechanistic support for nanocatalytic therapies targeting neuroinflammatory diseases [79]. Similar antioxidant enzyme-like activities of SACs can be applied not only to treating diseases like inflammation but also to medical sensing and disease monitoring [80,81]. Gao et al. have developed a multifunctional electrochemical sensing platform based on atomic engineering iron SAC (FeN_4), which realizes real-time detection of dopamine in the living brain without inflammatory interference. The catalyst has both high-efficiency antioxidant activity and excellent dopamine electrocatalytic oxidation performance. By eliminating ROS and neuroinflammation caused by electrode implantation, the accuracy and reliability of long-term neurochemical monitoring have been significantly improved. This method provides new ideas for the design of implantable devices with both anti-inflammatory and sensing functions, and promotes the application of SACs in the field of biomedical sensing [82].

The antioxidant enzyme-like activity of SACs can remove a large amount of reactive oxygen ROS in the body and convert it into harmless substances, inhibiting inflammatory reactions and improving the microenvironment. This characteristic makes it widely used in the field of biomedicine.

2.2.3. Other Enzymatic Activities and Synergistic Effects

In addition to the common enzyme-like activities involved in ROS metabolism mentioned above, researchers have also engineered SACs exhibiting other biological enzyme-like activities for biomedical applications. Furthermore, in complex physiological processes, the activity of a single enzyme is often insufficient to meet the needs. Therefore, SACs designed for biomedical applications often possess multiple enzyme activities simultaneously, participating in physiological processes together [83,84]. Xue et al. developed an Fe-N_3 SAC exhibiting outstanding SOD, CAT, ascorbate peroxidase (APx), and GPx activities. These enzyme-like activities form a complete antioxidant cascade reaction network, synergistically scavenging excess ROS in psoriatic lesions to fundamentally alleviate oxidative stress. Results indicate effective reduction in pro-inflammatory cytokine expression, inhibition of pathological epidermal hyperplasia, and restoration of skin homeostasis, demonstrating significant therapeutic efficacy in psoriasis treatment [85]. Beyond metallic SACs mimicking natural enzyme activity, recent studies demonstrate that non-metallic SACs can also emulate natural enzymes. For example, the non-metallic single-atom selenium (Se) nanoenzyme (SeSAE) constructed by Cheng et al. can mimic the activity of the natural NADPH oxidase, efficiently converting NADPH to $NADP^+$ and inducing the generation of ROS. NADPH, as a primary electron donor, plays a crucial role in maintaining cellular redox homeostasis and supporting anabolic processes. The NADPH oxidase activity of SeSAC leads to NADPH depletion, excessive accumulation of ROS, and disruption of antioxidant regeneration and essential biosynthetic pathways. Consequently, this interference compromises tumor compensatory mechanisms, impairs antioxidant defenses, and induces metabolic abnormalities and dysregulation, thereby inhibiting tumor progression [21].

The above demonstrates that a fundamental characteristic of SAC enzyme activity lies in its inherent multifunctional synergism. Unlike highly specific natural enzymes, a SAC often simultaneously mimics the activities of multiple natural enzymes such as OXD, POD, and so on [86,87]. This "one enzyme, multiple functions" property is not a simple accumulation of functions but constitutes a synergistic catalytic system. A common application is to use OXD activity to activate the reaction chain and activate oxygen molecules, while POD activity uses H_2O_2 to further produce more active free radicals. At the same time, POD activity quickly removes excess H_2O_2 to prevent inhibition of other reaction pathways. This ability to integrate and coordinate

multiple activities within a single active site enables SACs to adapt flexibly and efficiently to complex catalytic environments. Through multiple parallel pathways, they can complete complex catalytic tasks that cannot be achieved by a single enzyme, showing great application potential in the field of biomedicine [88–90].

2.3. Precision Control Strategies for Catalytic Activity

Although SACs have great potential due to their maximum atomic utilization and structural uniformity, their catalytic properties do not depend entirely on isolated metal centers. Atomic dispersion is only a prerequisite for high-efficiency catalysis. The final activity, selectivity and stability of the catalyst also depend on the complex interaction between single metal atoms and their surrounding microenvironment [91–93]. Therefore, how to accurately regulate the local electrons and geometric structure of single-atom active sites through reasonable strategies to enhance their catalytic activity is an important research hotspot in this field. This section focuses on the strategy of regulating catalytic activity, and elaborates on the following aspects.

2.3.1. Regulation of Intrinsic Properties of Metal Centers

In the multi-level regulation strategy of SACs, controlling the inherent properties of metal centers is the cornerstone and the first step in determining its catalytic properties. Directly select metal elements with specific electronic structures as active centers, so as to fundamentally pre-set the basic ability of catalysts to interact with reactants molecules [94].

Fei et al. explain the inherent regulation of metal centers in SACs at the paradigm level. They report a general approach to a series of atomic 3d metals embedded in nitrogen-doped holey graphene frameworks (M–NHGFs, M = Fe, Co or Ni). Through systematic X-ray absorption fine structure (XAFS) analysis and annular dark-field scanning transmission electron microscope (ADF-STEM) imaging, they confirmed for the first time that different metal centers are embedded in graphene double voids and have the same local coordination geometry. This shows that after eliminating interference factors such as the coordination environment and the carrier effect, the difference in the catalytic properties of the SACs can be attributed only to the different inherent electronic structures in the metal center. DFT calculations reveal that the oxygen evolution reaction (OER) pathway transitions from a single-site mechanism at Fe/Co centers to a dual-site mechanism at Ni centers due to the progressive increase in metal d-electron count. This results in a clear catalytic activity trend: Ni > Co > Fe. This trend was subsequently validated by electrochemical measurements, where Ni-NHGF exhibited outstanding oxygen evolution reaction activity and stability. This study successfully explored and quantitatively established the correlation between the atomic structure of the metal center and its catalytic performance, demonstrating a crucial step in rationally designing and synthesizing SACs with exceptional atomic utilization efficiency and catalytic activity (Figure 4) [95].

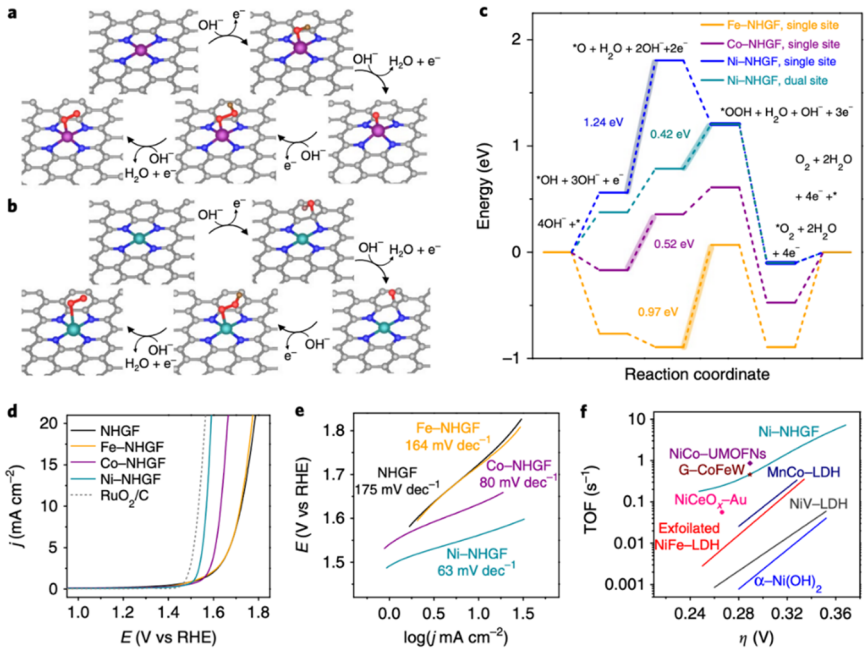

Figure 4. Evaluation of catalytic activity by DFT simulations and electrochemical measurements. (**a**,**b**) Proposed reaction scheme with the intermediates having optimized geometry of the single-site (**a**) and dual-site mechanisms

(**b**) towards OER. (**c**) Free energy diagram at 1.23 V for OER over Fe–NHGF, Co–NHGF and Ni–NHGF with a single-site mechanism, and Ni–NHGF with a dual-site mechanism. The highlights indicate the rate-determining step with the values of the limiting energy barrier labelled. (**d**) OER activity evaluated by LSV in 1 M Potassium hydroxide at a scan rate of 5 mV s^{-1} for NHGF, Fe–NHGF, Co–NHGF and Ni–NHGF along with a RuO_2/C catalyst as a reference point. The data are presented with current–resistance (iR) correction. (**e**) The Tafel plots of the corresponding catalysts shown in d. (**f**) Turnover frequency (TOF) values of the Ni–NHGF catalyst and other recently reported OER catalysts based on earth-abundant metals, including NiCo ultrathin metal–organic framework nanosheets (NiCo-UMOFNs), gelled CoFeW oxyhydroxides (G-FeCoW), cobalt–manganese layered double hydroxide (MnCo-LDH), NiCeOx-Au, exfoliated nickel-iron layered double hydroxide (NiFe-LDH), nickel-vanadium monolayer double hydroxide (NiV-LDH) and α-$Ni(OH)_2$. The TOF values are based on the total amounts of metal for all catalysts [95]. Copyright 2018, Springer Nature.

Thus, the selection of the metal center is not a simple element substitution but a rational design based on a profound understanding of the target reaction mechanism. It determines the theoretical upper limit of catalyst performance, while subsequent strategies such as coordination environment engineering and support regulation serve as further "fine-tuning" and optimization of activity to approach or even surpass this limit. In-depth research into the intrinsic properties of metals serves as the logical starting point for establishing the "structure-activity relationship" in SACs and achieving targeted catalyst design [96].

2.3.2. Coordination Environment Modulation

Coordination Number

Most SACs adopt M-Nx coordination structures (where M is a metal atom, and x is typically 4). However, the nonpolar coordination structure leads to symmetric electron distribution, resulting in insufficient adsorption capacity and catalytic activity. Altering the number of coordinating nitrogen atoms may break local charge symmetry, increase electron density at the metal center, and optimize adsorption strength with reaction intermediates [97]. Therefore, controlling the coordination number may be a key strategy for optimizing the electronic structure of SACs and thereby enhancing their intrinsic activity.

Song et al. clearly demonstrate the pivotal role of coordination number in determining the oxygen reduction reaction (ORR) activity of iron-based SACs. They prepared Fe-Nx/C catalysts via a simple nitric acid oxidation of carbon black method and ingeniously combined selective chemical etching with poisoning experiments to successfully distinguish the contributions of different active sites, including Fe-N_2, Fe-N_4, Fe_4-N-C, and N-C. Crucially, their theoretical and experimental results jointly established the catalytic activity hierarchy: Fe-N_2> Fe-N_4> Fe_4-N-C > N-C. This directly demonstrates that adjusting the coordination number between the Fe center and the N atom can alter the catalytic activity of a SAC [98]. On this basis, Shen et al. successfully synthesized a new catalyst by evenly dispersing a large number of highly active FeN_2 sites on the surface/edge of nitrogen-doped ordered mesoporous carbon (NOMC). Compared with the traditional FeN_4 structure, theoretical calculations show that due to the weak interaction between FeN_2 and intermediates and the enhanced electron transfer capacity, it shows better activity in ORR. This study established the linear relationship between ORR current density and FeN_2 site concentration for the first time, clearly proving that FeN_2 is the main active site, and confirming the high efficiency of FeN_2 position structure [99]. Similarly, Liang et al. systematically regulated a series of single-atomic cobalt catalysts with a specific Co-Nx (x = 2, 3, 4) structure for the peroxymonosulfate (PMS) activation. Their research directly reveals the negative correlation between catalytic specificity and the coordination number, and the activity order is: Co-N_2 > Co-N_3 > Co-N_4 [100]. The research by Song and Shen's team on the Fe-Nx system in the ORR and Liang's team on the Co-Nx system in PMS activation have revealed the pattern of low coordination number inducing high activity. However, the conclusion is not absolute. Liu et al. constructed an Ir-N_5 SAC that, compared with the traditional Ir-N_4 structure, introduced an axial nitrogen ligand to disrupt the original symmetrical electron distribution. This enhanced the adsorption and activation ability of the active site for the reaction substrate, endowing it with a variety of enzyme-like activities. Therefore, it can efficiently generate ROS in the tumor microenvironment and realize the cycling of the substrate between O_2 and H_2O_2 [101]. These studies indicate that there is no clear linear relationship between coordination number and catalytic activity in different SACs. Changes in coordination number affect the catalytic activity of the SAC by altering its electronic structure. These findings have deepened our understanding of the structure-activity relationship between electronic structure, adsorption behavior and catalytic activity, and also put forward clear requirements for future precise and controllable synthesis.

Type of Coordinating Atoms

In addition to the influence of the coordination number, the type of coordinating atom is also crucial for regulating the catalytic properties of SACs [102]. By replacing some nitrogen atoms in the traditional M-N_4 structure with heteroatoms with different electronegativity (such as sulfur and phosphorus), the symmetry of the coordination field can be effectively broken, thus causing charge redistribution, optimizing the adsorption behavior of reaction intermediates at active sites, and improving the catalytic performance [103–105].

In recent years, due to the low electronegativity (relative to nitrogen) of sulfur (S) and its stronger electron-ginding ability, it has been widely used as a common coordination heteroatom to regulate the electronic structure of metal centers [106]. Long et al. designed a composite catalyst composed of CoS nanoparticles and CoN_4S_1 SACs for high-efficiency hydrogenation of nitroaromatics. Theoretical calculations show that the introduction of S moves the d-band center of Co from −0.86 eV (CoN_4) to −1.24 eV (CoN_4S_1), which significantly weakens the adsorption strength of the reaction intermediate and alleviates the problem of overadsorption. This improves the activity and selectivity of the hydrogenation reaction. The study also shows that the CoN_4S_1 site shows excellent structural stability and remains intact after ten reaction cycles, while CoS nanoparticles aggregate, hydroxylation and dissolve, which further highlights the durability advantage of SACs [107]. Additionally, in the S-doped Fe-N-C nanoenzyme reported by Lu et al., the introduction of S formed Fe-N_4S_2 active centers. This not only reduced the adsorption energy of O_2 but also accelerated charge transfer between Fe and O, significantly enhancing its oxidase-mimetic activity. It was successfully applied for colorimetric detection and photothermal therapy of tumor cells [108].

Phosphorus (P) doping also plays a crucial role in regulating the electronic structure and catalytic performance of SACs [109–111]. Liu et al. successfully constructed Fe–N/P–C catalysts that demonstrated outstanding performance in the electrochemical reduction of CO_2 to CO. Here, P coordinates with Fe to form FeN_3P active sites, effectively lowering Fe's oxidation state and increasing its electron density. This optimizes CO_2 activation and adsorption of the key intermediate COOH. Simultaneously, P introduction significantly reduces the energy barrier of the rate-determining step in CO_2 reduction and weakens H adsorption, strongly suppressing hydrogen evolution side reactions. Furthermore, P doping enhances the structural stability of active sites, preventing Fe atom agglomeration and deactivation during the reaction. This study elucidates the effective mechanism by which the heteroatom P synergistically modulates the electronic structure and coordination environment to enhance the activity and selectivity of SACs [112]. To identify optimal coordination conditions, Zhang et al. systematically compared the effects of S and P doping on the peroxidase-like activity of cobalt-based single-atom nanozymes (SACNZs).The study revealed that S doping (Co–N_3S_1) more effectively modulates the electronic structure of Co compared to P doping (Co–N_3P_1) and pure N coordination (Co–N_4), lowering the energy barrier for ·OH generation. Consequently, it demonstrated optimal catalytic therapeutic effects in both in vitro antibacterial activity and in vivo wound healing [113].

The rational introduction of heteroatoms effectively modulates the local electronic structure of SACs, optimizing the adsorption/desorption behavior of intermediates and thereby achieving synergistic enhancement of catalytic activity and selectivity. This coordination engineering provides crucial theoretical foundations and practical pathways for the rational design of high-performance SACs.

2.3.3. Regulation of Support Interactions

The performance of SACs also depends on its support. In addition to anchoring and stabilizing isolated metal atoms, the support also enhances its catalytic activity, selectivity and stability by changing the electronic structure and configuration environment through complex metal-support interactions. According to the composition and structural characteristics, commonly used support systems can be divided into the following categories: oxide supports, carbon-based supports and metal organic frameworks (MOFs) or covalent organic frameworks (COFs). Different types of supports significantly regulate the activity and selectivity of SACs through mechanisms such as electronic effects, interface interaction and geometric domain limits.

Metal Oxide Supports

Metal oxide supports, such as TiO_2, CeO_2 and Fe_2O_3, are the most widely studied supports categories. These supports play a crucial role in determining the activity, selectivity and stability of SACs. Their impact is far more than a simple physical load, but atomic-level regulation is achieved through precise metal-carrier interaction [26,114–119].

As a carrier, CeO_2 is widely used in SACs systems, which can affect the catalytic activity of SACs through different effects. Hu et al. proved that the (100) crystal surface of CeO_2 can prioritize the stability of Pd single atoms because it is easy to form abundant oxygen voids. This forms a highly active Pd-O coordination structure,

so that in the N-alkylation reaction, its selectivity is significantly better than the (111) crystal surface of Pd cluster aggregation. This shows that basal surface engineering is crucial to regulating the single atomic electron state and reaction path (Figure 5a,b) [120]. At the same time, Fu et al. found that catalysts where Pt single atoms and Pt nanoparticles coexist showed the best performance in CO oxidation reactions. This is because Pt single atom, as a regulatory site, can change the reaction potential barrier of the lattice oxygen on the surface of the adjacent CeO_2 carrier, and these two components have a significant synergistic effect under the mediation of the carrier. This suggests that the form in which metals exist on the support is not fixed, and advanced preparation methods can precisely control the ratio of single atoms to nanoparticles to achieve better catalytic effects (Figure 5c,d) [121]. Additionally, Pham, H. N. et al. discovered that the macrostructural stability of the support directly determines the practical application potential of SACs. Pure CeO_2 readily sintered at high temperatures, causing a drastic reduction in surface area. However, constructing a composite support by combining it with high-surface-area Al_2O_3 not only effectively preserved the atomic capture capability of CeO_2 nanocrystals but also significantly enhanced the overall thermal stability of the material. This enabled the maintenance of highly dispersed single-atom states and excellent low-temperature catalytic activity even under harsh conditions (Figure 5e,f) [122].

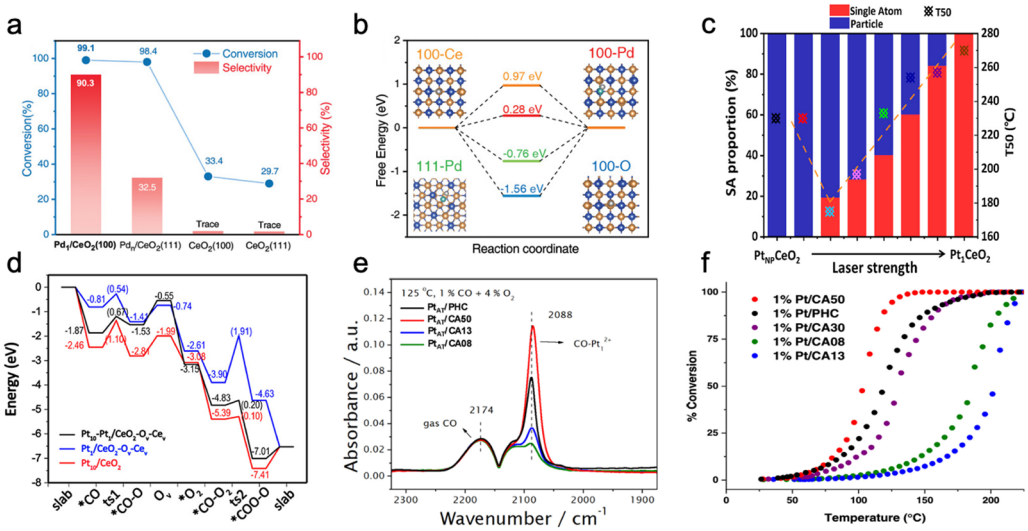

Figure 5. (**a**) Comparison of conversion and selectivity over different catalysts. (**b**) DFT calculation results for hydrogen atom adsorption free energy on different sites [120]. Copyright 2022, John Wiley and Sons. (**c**) Relationship between the Pt1 proportion, T50, and laser ablation strength. (**d**) computed energies of intermediates and transition states for Pt_1/CeO_2-O_v-Ce_v, Pt_{10}/CeO_2, and Pt_{10}–Pt_1/CeO_2-O_v-Ce_v [121]. Copyright 2023, American Chemical Society. (**e**) CO-DRIFTS of 1 wt % PtAT/ceria-alumina and PtAT/PHC ceria catalysts. (**f**) CO oxidation on 1 wt % PtAT/ceria-alumina and PtAT/ceria catalysts after reduction in flowing CO. Data plotted are for the third run. The improved performance of PtAT/CA50 can be attributed to smaller crystallites of ceria on the alumina, providing a higher surface area and more facile oxygen transfer to the Pt metal crystallites formed during reduction [122]. Copyright 2022, American Chemical Society.

Metal oxide carriers affect the performance of SACs on all scales from atoms to macro through their crystal surface structure, defective chemical properties and dynamic synergy with metal species. This provides some guidance for the reasonable design of high-efficiency and stable SACs.

Ordered Porous Materials

Ordered porous materials show unique advantages in the construction of SACs because of their adjustable pore structure, abundant surface coordination sites and excellent stability [123]. Among them, zeolites and MOFs are served as two typical ordered porous carriers. They can significantly improve the activity, selectivity and stability of SACs through the spatial limit effect and electronic structure regulation [124–126].

Zeolite has a highly ordered crystal skeleton and nanoscale cage-shaped hole structure. Its rigid micropores effectively prevent single-atom migration and aggregation, which is conducive to stable atomic dispersion. The abundant oxygen atoms and adjustable acidic sites in the zeolite skeleton form a strong interaction with the metal, resulting in the formation of a stable M-O-Si configuration structure in a limited space. This optimizes the energy distribution of adsorption and reaction intermediates [127]. Chen et al. selectively limited Pt single atoms to the

cage-shaped cavity of Y-type zeolite, achieving high selectivity and anti-poisoning ability for hydrogenation. Theoretical calculations show that the strong electric field and rigid space constraints inside zeolite change the electron occupancy rate of the metal d orbit, thus accurately regulating the electron structure and reaction path of the active site [128]. Similarly, Liu et al. observed that the single atoms anchored by zeolite showed better electron transfer efficiency and reaction selectivity than traditional catalysts in hydrogenation/dehydrogenation reactions, which was attributed to the strong restriction effect and stable geometric environment provided by the ordered channel [126].

MOFs stand out as a new ordered porous material, with high specific surface area, flexible pore structure and adjustable organic-inorganic dual-compont characteristics. The metal nodes and organic ligands in MOFs can achieve the precise construction of SACs on the atomic scale. By adjusting the valence state and local charge density of the metal, the single atom center can be given excellent catalytic activity [129–131]. Yu et al. synthesize MOF-based SACs at room temperature to stabilize the metal center and achieve efficient oxidation reactions [132]. Xue et al. further studied the mechanism of CO oxidation on MOF-808-M^{2+} (M = Zn, Cu, Fe, Pd, Ni, Pt) through DFT and microdynamic analysis. The results show that the Zr_6O_8 node in MOF-808 provides a stable triple M-O-Zr anchor positioning point for metal single atoms. Among them, Pt^{2+} shows the highest stability and electron receptor ability, and can efficiently activate CO and O_2 through the Langmuir-Hinshelwood mechanism. This significantly reduces the reaction energy barrier and achieves the highest turnover frequency. The synergistic electronic interaction between MOF organic ligands and inorganic nodes can flexibly regulate the adsorption energy and reaction energy barrier, which is in line with the principle of optimal balance between adsorption and desorption in Sabatier's principle [133].

As typical ordered porous materials, zeolites and MOFs embody two single-atom activity regulation modes: rigid restriction and flexible regulation. Zeolite enhances the structural stability and reaction selectivity of single atoms through spatial constraints and frame electric fields, while MOFs use the designability of colocation chemistry to finely regulate the single atomic electron structure and reaction path. Both of these materials enhance the synergy of the metal-carrier interface at the atomic scale, significantly improving the activity and durability of SACs. Future research can explore the combination of zeolite stability and the programmability of MOF to achieve precise control of the single-atom catalysis process.

Other Two-Dimensional Material Supports

In addition to metal oxides and ordered porous materials, new two-dimensional materials, such as graphite carbon nitride (g-C_3N_4) and metal carbides, nitrides, or carbon-nitrides (named MXenes), provide an excellent anchoring platform for SACs due to their unique electronic structure and surface chemical properties. Compared with three-dimensional carriers, these two-dimensional materials have high specific surface area, short charge transmission path and adjustable colocation environment, which helps to clarify the structure-performance relationship more clearly [134,135].

Take g-C_3N_4 as an example, the hexagonal cavity in its nitrogen-rich skeleton is the ideal site for anchoring a single atom. However, the recent research of Zhao et al. has deepened our understanding of this "anchoring" mechanism: they calculated through DFT that the migration of a single atom Pt on the g-C_3N_4 plane shows anisotropy. On a global scale, due to the limitations of high energy barriers, this migration has high stability and effectively prevents long-range migration and reunion. However, on the local scale of a single cavity, atoms can easily gather dynamically to form clusters. This shows that the precise control of the metal load below the density of the hexagonal cavity is crucial for the preparation of stable SACs [135]. In addition, the powerful electronic regulation ability of g-C_3N_4 makes it an ideal design platform for high-performance catalysts. Lv et al. found through systematic calculation and screening that the d-band center of the anchored single-atom transition metal (such as Ru, Pt) is the key activity descriptor; for example, in the electrocatalytic nitrate reduction reaction (NO_3RR), Ru/g-C_3N_4 achieves the best NO_3^- due to its moderate d-band center, whose limit potential is significantly better than that of many reference catalysts, showing excellent activity and selectivity [136]. At the same time, Xu et al. also studied the morphological effect of g-C_3N_4 carriers. Through the experimental synthesis of curved g-C_3N_4 nanorods (about 9 nm in diameter), the traditional plane model was broken through, revealing that its curvature effect could expand the layer spacing and induce the anchored Co single atoms to form a low-colocation structure. This unique local environment significantly enhances the adsorption of reactants, reduces the dissolving energy barrier of O_2, and achieves a high conversion rate of 22.4% and selectivity of more than 95% in the cyclohexane oxidation reaction. This highlights the surface engineering as a previously neglected but very effective regulatory method [137]. Similar MXenes, with their high conductivity and tunable surface functional groups, also provide efficient electron transport pathways for single atoms [134,138].

2.3.4. Control of Dual-Atom Sites

In dual-atom SACs, the introduction of a second atom fundamentally reconfigures the electronic and geometric microenvironment around the single-atom site through a "paired site + shared ligand" mechanism, thereby overcoming the scaling limitations on activity and selectivity inherent in SACs [139,140]. On one hand, metal–metal or metal–nonmetal interactions induce significant charge redistribution and spin state modulation, pulling the adsorption energy of key intermediates from "excessively strong" or "excessively weak" back to the optimal range. Chen et al. introduced Se single atoms into Fe–N–C to construct Fe_1Se_1-NC. Se serves as a new ORR active site while inducing charge rearrangement and spin state regulation at Fe sites. Consequently, ORR activity in both acidic and basic electrolytes significantly outperforms that of Fe_1-NC and Se_1-NC, demonstrating a typical binuclear synergistic effect [141]. On the other hand, adjacent bimetallic sites can synergistically adsorb/activate reactants through spatial "soft association." For instance, in FeZn-NSC—where Fe/Zn dual single atoms are anchored on N/S co-doped hollow carbon polyhedra and carbon nanotubes—where proximate $Fe–N_4$ and $Zn–N_4$ sites form favorable electronic coupling and intermediate-sharing adsorption under S-doping regulation, elevating the ORR half-wave potential to 0.87 V—surpassing Pt/C. This demonstrates that bimetallic pairs can significantly enhance conversion efficiency by synergistically modulating local electronic structures and exposing more accessible sites relative to SACs [142]. Furthermore, Gao et al. noted in their review on microenvironment engineering that introducing bridging heteroatoms such as O or N between diatomic centers to construct W–O–Mo, Ni–O–Fe structures, the bridging atoms provide additional M–X–M active frameworks while establishing efficient charge/spin transport pathways between the two metals. This makes it possible to accurately control the valence state and adsorption configuration of the metal center, thus significantly reducing the free energy barrier of key steps such as hydrogenation reaction (HER) and oxygenation reaction (OER) [143]. In a word, the transformation from diatom to single-atom enables the precise regulation of single-atom active sites through metal-metal/metal-non-metallic synergy, charge and spin reconstruction, and the regulation of the microenvironment by bridge ligands without affecting the atomic utilization rate. This provides an important idea for promoting the design of high-efficiency single-atom catalysis system.

3. Applications of Single-Atom Catalysts in Biomedical Fields

With its high-efficiency enzyme-like activity and excellent biocompatibility, SACs have broad application prospects in biomedicine, environmental monitoring and other fields. In the field of biosensing, SACs can be used as high-sensitivity and high-selectivity signaling amplifiers for the detection of glucose, nucleic acid and disease biomarkers. In the field of antibacterial treatment, SACs can efficiently kill drug-resistant bacteria under low concentration H_2O_2 conditions through photothermal/catalytic coordination strategies, and promote the healing of infected wounds. In addition, the application of SACs in antioxidant treatment, tumor catalytic treatment and degradation of environmental pollutants has also attracted much attention. In the future, in-depth research on the relationship between SACs and their interaction with biological systems is expected to build a more bionic intelligent catalytic diagnosis and treatment integration platform.

3.1. Catalytic Cancer Therapy

Although traditional cancer treatments such as chemotherapy and immunotherapy have achieved remarkable results, tumors remain the main causes of morbidity and mortality. The current tumor treatment faces many challenges, including the therapeutic bottleneck caused by tumor heterogeneity and drug resistance, and the uneven distribution of clinical medical resources [144,145]. SACs provide new solutions to these challenges. Its atomic dispersion structure achieves nearly 100% atomic utilization rate and extremely high catalytic efficiency, so that it can accurately regulate the tumor microenvironment. As a multi-functional platform, they can work together with radiotherapy, immunotherapy and other therapies to improve the overall therapeutic effect, representing an important frontier exploration in promoting the development of tumor treatment in a more accurate, efficient and controllable direction [56,146].

Due to its highest atomic utilization rate, clear active site and adjustable catalytic properties, SACs have become the forefront of tumor catalytic medicine [147]. Their core mechanisms for tumor treatment include(Figure 6): (1) Depletion of glutathione: Catalytically oxidizing and consuming glutathione—the primary antioxidant in tumor cells—weakens their defense capabilities and amplifies oxidative stress; (2) Alleviation of tumor hypoxia: Catalytically decomposing hydrogen peroxide to produce oxygen, improving tumor hypoxia and thereby enhancing the efficacy of radiotherapy and photodynamic therapy; (3) Mimicking natural enzyme functions: Precisely mimicking the atomic structures of key enzymes like peroxidase to trigger specific catalytic reactions at

tumor sites; (4) Synergistic combination therapy: Acting as a highly efficient catalyst when combined with SDT, RT, and PTT to produce synergistically enhanced antitumor effects [148–150].

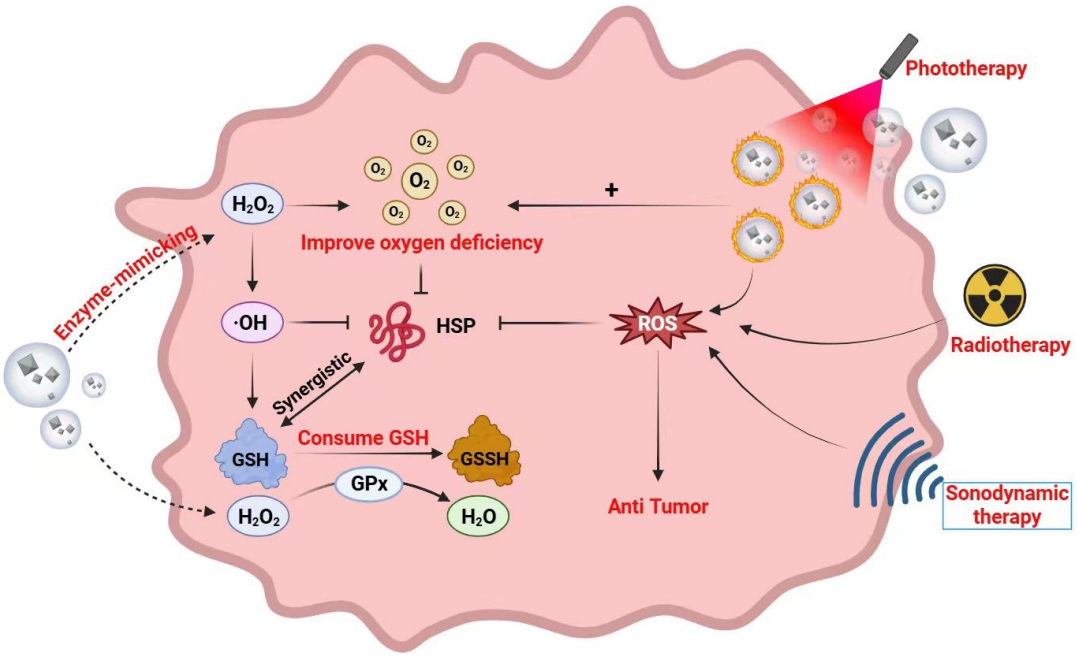

Figure 6. Schematic illustration of SACs mechanisms for tumor treatment. Created with BioRender.com.

SACs employed for tumor therapy often rely solely on their catalytic activity. However, by modulating the catalytic reaction process, researchers have designed diverse highly efficient SACs featuring different substrates and structures [151–153]. For instance, to broaden substrate scope, Wang et al. developed a mesoporous hollow copper SACs, which no longer relies only on the limited H_2O_2 in the tumor. On the contrary, it uses loaded calcium peroxide (CaO_2) to provide H_2O_2 in situ in the tumor microenvironment. At the same time, the released calcium ions will cause mitochondrial "calcium overload" and bind to the ROS produced by the copper single-atom, producing a double killing effect through oxidative stress and ion disturbance. This establishes a self-amplifying synergistic therapeutic system [154]. Similarly, to enhance catalytic killing effects, Zhao et al. designed an iron-cobalt bimetallic dissociative SAC (FeCo-DIA/NC). Its core innovation lies in proposing an atomic-level "division of labor and synergy" mechanism: where iron atoms primarily catalyze Fenton reactions to generate ROS, while cobalt atoms mainly catalyze Fenton-like reactions to produce singlet oxygen. These ROS can interconvert and regenerate H_2O_2 within acidic microenvironments, forming an efficient "ROS cycle" that significantly amplifies the catalytic killing effect [155].

To achieve superior therapeutic outcomes, a SAC is typically engineered as a highly efficient antitumor composite platform where multiple synergistic functions converge. These include the catalytic activity of the SAC, the physical properties of the platform structure, and the pharmacological effects of the loaded drug [156–158]. Some efficient antitumor composite platforms are listed in Table 1. Cheng et al. designed the iridium SAC, simultaneously mimicking the dual activities of POD and glutathione peroxidase (GSHOx): In the acidic tumor microenvironment, it catalyzes endogenous H_2O_2 to generate highly toxic hydroxyl radicals (·OH) while simultaneously depleting the key antioxidant glutathione (GSH), thereby disrupting the redox balance of tumor cells. To enhance efficacy, researchers further developed a composite nanoplatform (Pt@IrSAC/RBC) loaded with a platinum (IV) prodrug capable of capturing GSH (Figure 7). This platform was encapsulated with red blood cell (RBC) membranes to improve biocompatibility and prolong circulation. It also efficiently induces ferroptosis in tumor cells while exhibiting superior photothermal properties. Ultimately, in a triple-negative breast cancer mouse model, a single treatment combined with near-infrared laser irradiation achieved complete tumor ablation without recurrence, while demonstrating good biosafety. This study provides new insights for designing highly effective, low-toxicity novel nanocatalytic antitumor agents [159]. Various systems, such as nitrogen-doped jellyfish-like mesoporous carbon nanomotors (JMCNs) loaded with copper single atoms (Cu- JMCNs) and manganese-doped single-atom nanoenzyme composite metal-organic frameworks, achieve potent antitumor effects through synergistic multi-mechanistic actions [160–163].

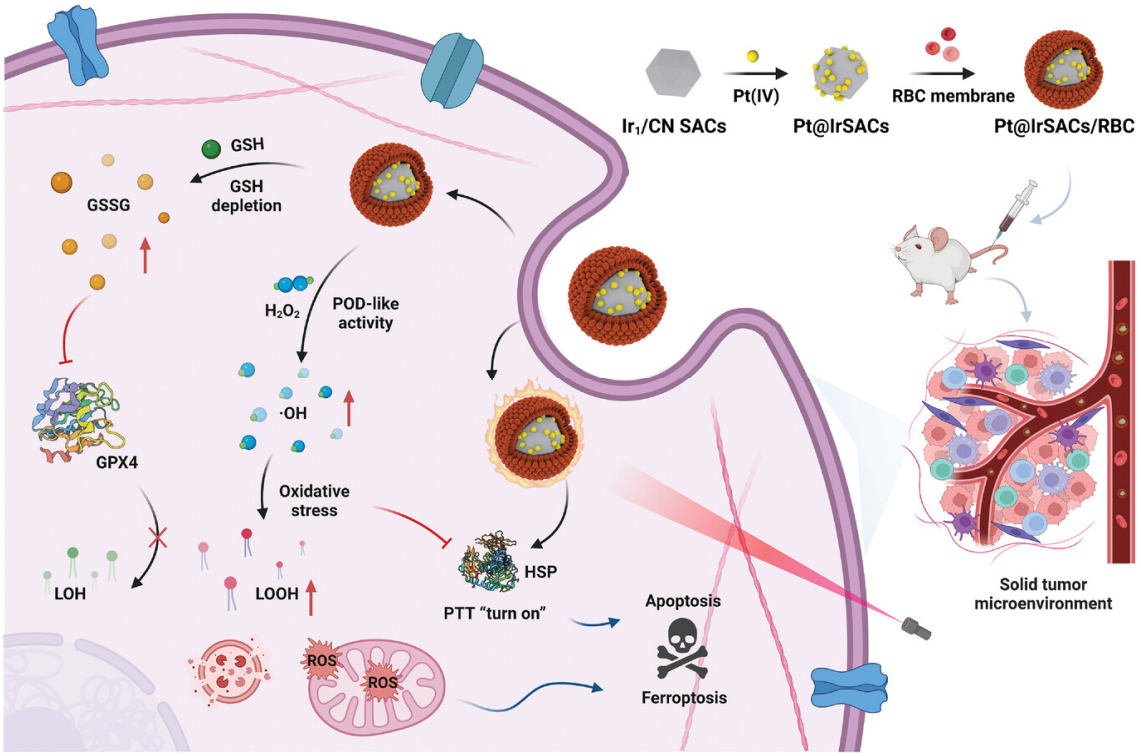

Figure 7. Schematic illustration of Pt@IrSAC/RBC application in tumor ferroptosis therapy [159]. Copyright 2023, John Wiley and Sons.

Photothermal therapy(PTT), as a novel therapy that is spatiotemporally controllable, minimally invasive, and highly selective, has become a major tumor treatment method after surgery, radiotherapy, and chemotherapy by using different excitation sources to increase the local temperature of cancerous tissue to achieve tumor ablation [164]. Therefore, many SACs have achieved synergistic killing of tumor cells by utilizing the photothermal effect of the carrier. For example, Zhou et al. designed a MOF rich in porphyrin-like single atom Fe(III) centers (P-MOF), which exhibits excellent photothermal effect under near-infrared light (808 nm) irradiation, achieving a photothermal conversion efficiency of up to 41%, which is significantly better than traditional photothermal materials, realizing photodynamic therapy, and catalyzing the decomposition of endogenous hydrogen peroxide in tumors into oxygen, improving the hypoxic microenvironment of tumors. It has shown good anti-tumor effects and biosafety in in vivo and in vitro experiments [165]. Although traditional high-temperature PTT has a definite curative effect, high temperature can easily cause thermal damage to normal tissues. Therefore, people began to explore low-temperature PTT, but the existence of heat shock proteins (HSPs) limited the application of low-temperature PTT. Based on this, Chang et al. proposed an innovative strategy: ferroptosis-enhanced mild PTT based on SACs. They designed and synthesized nitrogen-doped carbon-supported palladium SACs, which exhibited excellent photothermal performance under 1064 nm light irradiation. Utilizing its unique dual activities of POD and GSHOx properties, it can induce a large accumulation of lipid peroxides and ROS in the tumor microenvironment, triggering ferroptosis and effectively cleaving HSPs. This breaks through the key bottleneck of tumor heat tolerance in mild temperature photothermal therapy (38–43 °C), achieving low-temperature high-efficiency treatment while maximizing the protection of surrounding normal tissues [166]. More and more studies have shown that SACs based on carbon materials are a new type of multifunctional photothermal agent (i.e., the common M-C-N structure), which can achieve low-temperature PTT without excessive reliance on the carrier, but through its POD-like enzyme activity, thus avoiding damage to surrounding normal tissues at high temperatures while fighting tumors [167]. Therefore, when designing a SAC for synergistic PTT against tumors, one could consider designing an M-C-N catalyst with POD enzyme activity. Furthermore, it can be modified according to specific targeting and chemotherapy requirements.

The antitumor effects of SACs are not only attributed to ROS-mediated killing but also commonly involve pathways such as copper death or ferroptosis, which rely on metal ion accumulation effects [168–170]. Vanadium-based SAC not only catalyzes endogenous H_2O_2 to generate ·OH but also induces mitochondrial copper metabolism disruption by downregulating acyl-CoA synthetase and dihydrolipoamide S-acetyltransferase expression, thereby triggering copper death. Simultaneously, it synergistically induces ferroptosis by depleting glutathione and inhibiting GPX4 activity [171]. Furthermore, to enhance ferroptosis efficacy, the cobalt-loaded

iron-based zeolite imidazolate framework material designed by Xu et al. demonstrated promising in vivo and in vitro antitumor effects and biosafety in colorectal cancer treatment. It not only induces ferroptosis by depleting glutathione and inhibiting GPX4 but also reduces tumor cell resistance to ferroptosis by downregulating the JAK1-STAT3 signaling pathway [172].

In summary, the development of SACs is evolving from an efficient "catalytic core" into a powerful "synergistic platform." With the aid of novel tools such as machine learning, it is becoming increasingly effective to construct composite platforms of SACs for disease treatment [173]. By deeply integrating with multiple technologies such as immunotherapy, kinetic systems, drug delivery, and diagnostic imaging, it holds promise for establishing a new paradigm of tumor therapy that integrates precision, efficiency, and safety, demonstrating immense clinical application potential.

Table 1. Details of some efficient antitumor composite platform.

Cancer Type	Therapeutic Modality	Representative Material	Key Performance Metrics	Applicable Scenario & Limitations
Non-small cell lung Cancer	Chemodynamic Therapy (CDT)	Fe-SAC [158]	~70% cell inhibition (24 h + 800 μg/mL)	Tailored for H_2O_2-overexpressing TME
Malignant Melanoma	Chemodynamic Therapy (CDT)	OsCu-Ov@CCM [174]	~75% cell inhibition (8 h + 40 μg/mL)	Synergy overcomes the activity limit of single-metal sites
Breast Cancer	Photothermal Therapy (PTT)	Cu-JMCNs [163]	~80% cell inhibition (4 h + 50 μg/mL + NIR)	d-orbital of Cu for efficient light absorption
	Sonodynamic Therapy (SDT)	PdSA/$Ti_{3-x}C_2T$_y [156]	~80% cell inhibition (24 h + 400 μg/mL + US)	Conductive support enhances US energy conversion
	Sonodynamic Therapy (SDT)	Zn/Pt SATs [175]	~90% cell inhibition (24 h + 400 μg/mL + US)	Electronic modulation optimizes H_2O_2 activation pathway
	Radiodynamic Therapy (RDT)	MCCP [176]	~80% cell inhibition (24 h + 50 μg/mL + X-ray)	Leverages deep tissue penetration of X-rays and catalytic amplification of SACs for "radio-catalytic" synergy.
Cervical Cancer	Photothermal Therapy (PTT)	PSMCA [160]	~60% cell inhibition (200 μg/mL + NIR)	Combinatorial killing via heat and ROS
	Photothermal Therapy (PTT)	PmMn/SAE [177]	~84% cell inhibition (3 h+400 μg/mL + NIR)	Carrier engineering optimizes light utilization and charge separation
	Photothermal Therapy (PTT)	C_3N_4-Mn [178]	~80% cell inhibition (12 h + 10 μg/mL + IR)	
Colon Cancer	Sonodynamic Therapy (SDT)	W-BN@Fht@TSCM [179]	~55% cell inhibition (12 h + 100 μg/mL + US)	Atomic doping tunes bandgap for enhanced sono-sensitivity

3.2. Anti-Inflammatory Therapy via ROS Scavenging

ROS are inevitable byproducts of daily biochemical and physiological processes in aerobic organisms. The antioxidant systems present within the body eliminate excess ROS, maintaining normal ROS levels in living organisms [180]. During inflammatory responses, immune cells generate large amounts of ROS to eliminate pathogens. However, an imbalance between ROS production and antioxidant systems can lead to excessive ROS oxidizing and damaging cellular components. This further activates core inflammatory signaling pathways like NF-κB, triggering the release of additional inflammatory mediators that exacerbate inflammation and cause tissue damage [181,182]. Existing anti-inflammatory therapies primarily target downstream components of this cycle. For instance, nonsteroidal anti-inflammatory drugs (NSAIDs) or biologics "interrupt" inflammatory signaling by inhibiting cyclooxygenase or blocking specific cytokines like TNF-α. However, they fail to effectively eliminate upstream ROS, which drive the cycle. This "symptom-relieving but not root-cause-treating" approach, coupled with potential systemic side effects like gastrointestinal damage and immunosuppression, limits their efficacy against chronic, refractory inflammation [183].

The core advantage and therapeutic mechanism of SACs lie precisely in directly breaking this vicious cycle. Their atomically dispersed metal active sites efficiently mimic the catalytic functions of natural antioxidant enzymes like SOD and CAT, rapidly converting excess harmful ROS into harmless substances like water or oxygen at the site of inflammation. This precise catalytic scavenging not only eliminates oxidative stress at its source and blocks the sustained activation of inflammatory pathways by ROS, but also protects surrounding tissues [184]. Its ROS-clearing anti-inflammatory action rests on three pillars: (1) Efficiently eliminating excess ROS through Fenton-like or cascade catalytic reactions, converting harmful ROS like superoxide anion ($O_2^{\bullet -}$), H_2O_2, and •OH into harmless water and oxygen, directly alleviating oxidative stress—this constitutes catalytic clearance; (2) Precise targeted delivery: Functional modifications to the surface of SACs enable them to utilize "cell hitchhiking" or active targeting strategies to accumulate in diseased tissues such as inflammatory sites, achieving in situ catalytic therapy while minimizing side effects on normal tissues; (3) Regulation of the immune microenvironment: By scavenging ROS, modulating hypoxia, and generating signaling molecules, SACs influence immune cell function and polarization, shifting them from pro-inflammatory to anti-inflammatory phenotypes. This indirectly suppresses inflammation and promotes tissue repair [185–187]. Qiao et al. designed the novel multifunctional bio-nanoplatform, combining dual SACs (DACs) with genetically engineered probiotic Escherichia coli Nissle 1917 (EcN) for synergistic treatment of ulcerative colitis (UC).The engineered bacteria stably express interleukin-18 binding protein (IL-18BP), which neutralizes pro-inflammatory cytokines; while DACs effectively scavenge intestinal ROS by mimicking multiple antioxidant enzyme activities. Following combined oral administration, this approach demonstrated significant therapeutic efficacy in a DSS-induced mouse colitis model: alleviating inflammatory symptoms, reducing ROS levels, repairing the intestinal barrier, and restoring gut microbiota richness and diversity. This platform achieves synergistic effects through ROS scavenging, immune modulation, and microbiome restoration, offering a novel multi-target therapeutic strategy for ulcerative colitis [76].

SACs regulate not only common inflammatory signaling pathways and molecules such as the NF-κB pathway and NLRP3 inflammasome, but also specific pathways closely associated with certain diseases to achieve therapeutic effects [188]. For example, Shi et al. developed isolated Cu_1-N_4 site SACs anchored on carbon supports for cascade catalytic treatment of atopic dermatitis (AD). This catalyst simultaneously mimics multiple enzymatic activities, effectively eliminating excess ROS at the lesion site. Crucially, transcriptomic analysis revealed for the first time that its therapeutic mechanism is closely linked to activating the PPARα/β-δ signaling pathway—suppressed in AD—which regulates oxidative stress to inhibit inflammation [189].

Simultaneously, the catalytic activity of SACs can be combined with physical effects such as near-infrared light and ultrasound to enhance anti-inflammatory therapeutic outcomes [190]. For instance, Xiang et al. designed a near-infrared light-enhanced platinum single atom/graphitic phase carbon nitride nanozyme for treating osteoarthritis. This Pt SAC not only efficiently scavenges ROS by mimicking SOD and CAT, but also achieves controllable synergistic amplification of catalytic activity and therapeutic efficacy through the photothermal enhancement effect induced by NIR-II laser irradiation. It demonstrates remarkable potential for reversing cartilage damage in both in vitro and in vivo experiments [191]. SACs achieve multi-pathway, synergistic intervention in the inflammatory microenvironment through their exceptional catalytic performance, demonstrating significant potential for clinical translation.

3.3. Antimicrobial and Wound Repair

Traditional antimicrobial approaches (e.g., broad-spectrum antibiotics) face limitations such as inducing bacterial resistance, disrupting normal microbiota, and having limited efficacy against biofilms. The escalating antibiotic resistance crisis and emerging infectious diseases urgently demand novel, non-antibiotic-dependent broad-spectrum anti-infective technologies. SACs, as novel nanozymes, possess highly efficient and controllable catalytic activity due to their atomically dispersed active sites. They can precisely eliminate bacteria by generating ROS through enzyme-like reactions while being less prone to inducing resistance. Their multifunctionality and designable targeting capabilities offer highly promising new strategies for combating drug-resistant bacteria and stubborn biofilm infections [192,193]. Researchers have designed SACs such as Fe SA/NPCs, Cu SAzyme, and Co-NC SAzyme to catalyze ROS production for bactericidal effects [194–196].

Recent research advances highlight a deepening trend in this field, shifting from single antimicrobial functions toward "multimodal synergistic treatment" and "adaptability to complex environments" [197]. The Pt single-atom-anchored Ti_3C_2 MXene nanoplatform (Pt-Ti_3C_2) demonstrates an exceptional synergistic antibacterial strategy: Pt sites confer peroxidase-like activity, catalyzing endogenous H_2O_2 to generate highly toxic ·OH; while the MXene carrier's superior photothermal effect not only physically kills pathogens but, more critically, significantly enhances the former's catalytic kinetics, achieving a photothermal-catalytic cascade amplification effect. This makes the effective removal of drug-resistant bacterial infection in deep tissues and the disintegration of biofilms is possible [198]. In addition, the therapeutic significance of SACs is not limited to the removal of pathogens, but also includes regulating the infected microenvironment and promoting tissue regeneration. Zhang et al. designed a new type of manganese-iron atomic catalyst (Mn/Fe SACs). In the catalyst, iron single atom (Fe-N_4) acts as a high-efficiency peroxidase to catalyze the conversion of hydrogen peroxide in the wound microenvironment into hydroxyl free radicals with strong bactericidal activity. At the same time, manganese single atom (Mn-N_4), as a hydrogen peroxide enzyme, decomposes hydrogen peroxide into oxygen, thus alleviating tissue hypoxia and transporting the catalyst to deeper infected sites. At the same time, it also shows glutathione oxidase activity and consumes the antioxidant glutathione, otherwise glutathione will reduce its bactericidal effect. This multifunctional synergy not only achieves a broad-spectrum sterilization effect of up to 95% in vitro, but also significantly accelerates wound healing and abscess regression in animal models through strong bactericidal activity, immunoregulation and promotion of angiogenesis, and integrates the functions from sterilization to promoting healing [199]. The study of SACs for the treatment of diabetic foot provides new ideas for managing this difficult chronic disease [200,201]. Dai et al. designed an intelligent nano-catalytic platform for diabetic wound healing. The platform is constructed by encapsulating copper-doped carbon point SACs (Cu/C-dots) with a variety of antioxidant enzyme activities in a ZIF-8 metal organic framework. In the diabetic rat model, the platform significantly accelerated the healing of the entire skin wound by promoting antibacterial, anti-inflammatory, angiogenesis and collagen deposition effects [202].

In the face of complex practical applications, the design concept of SACs shows excellent environmental adaptability. Wang et al. developed a silver single atom photocatalyst (Ag_1/ZIF) uniformly loaded on the metal organic framework ZIF-8-NH_2. Under low light irradiation, the catalyst can quickly generate ·OH free radicals and promote photo-induced electron transfer, thus efficiently inactivating E. coli, Staphylococcus aureus and viruses. The catalyst is integrated into the non-woven layer of the mask to give the mask excellent self-disinfection ability. In addition, the catalyst also shows potential application value in aerosol purification devices, providing new ideas for sustainable and efficient photocatalytic antibacterial technology [203]. In order to solve the core problem that traditional personal protective equipment (PPE) cannot effectively inactivate intercepted microorganisms, resulting in cross-contamination, Jin et al. proposed an innovative solution: integrating oxidase-like SACs into PPE. Take the atomically dispersed copper SACs (Cu-SAC) as an example, these materials can spontaneously and continuously convert ambient oxygen into ROS with strong bactericidal activity without external stimulation. This intrinsic, self-driven catalytic sterilization mechanism gives fiber membranes or plastic surfaces containing Cu-SAC strong and lasting broad-spectrum antibacterial ability. It has successfully upgraded the traditional physical barrier to intelligent protective equipment that can actively eliminate pathogens, providing a feasible technical way for the development of the next generation of self-antibacterial PPE [204].

The application of SACs in the field of infection control is rapidly developing in the direction of functional integration, mechanism optimization and diversified applications. Through the precise design of the metal-carrier interface, its catalytic performance and biological function can be customized, providing a promising platform for enabling an efficient, safe and adaptable next-generation infection control strategy.

3.4. Biosensing and Disease Diagnosis

In the field of life science and clinical medicine, the realization of high sensitivity and highly selective biomarker detection and effective intervention in major diseases are the keys to achieving precision medicine. Existing biosensors often face challenges such as insufficient sensitivity, dependence on expensive and unstable natural enzymes, and limited anti-interference ability when detecting ultra-low concentration biomarkers. However, SACs can be integrated into sensors as ultra-active and stable nano-art-enzymes due to their atomically dispersed metal active sites. Its core mechanism is that after identifying the target (such as glucose, DNA, tumor markers), it can efficiently catalyze colorimetric or electrolytic reactions. This significantly amplifies the weak identification signal and converts it into a strong signal, thus achieving ultra-sensitivity, high selectivity and rapid detection of trace targets, while greatly reducing the complexity and cost of the sensor [205].

Maintaining an appropriate blood sugar level is crucial to human health, and diabetics need long-term blood sugar monitoring. In the commonly used enzyme-based electrochemical detection methods, the core glucose oxidase is highly sensitive to temperature, humidity and pH, and is easy to inactivate. As a result, the storage conditions of the test paper are harsh, the shelf life is short and the operation time-consuming [206]. However, as an artificial enzyme, SACs can maintain catalytic activity even under harsh conditions and oxidize glucose molecules on the electrode surface. Its clearly structured active site provides the best adsorption and reaction site for glucose molecules, thus realizing the direct, efficient and highly selective electrooxidation of glucose [207]. Qi et al. have designed and synthesized a nickel-selenium atomic catalyst (Ni_1Se_1/NC). The catalyst has adjacent Ni-N_4 and Se-C_3 sites and can be used for high-sensitivity enzyme-free electrochemical glucose sensing. Research shows that nickel single-atoms are the main active sites of glucose oxidation, and although adjacent selenium single-atoms do not have catalytic activity themselves, their electron structure can be regulated by attracting electrons from nickel sites. This electron effect enhances the adsorption of glucose at the nickel site and accelerates the electron transfer rate, thus significantly improving the electrocatalytic oxidation activity of glucose. This work reveals a new coordination mechanism, that is, non-catalytic atomic sites enhance adjacent active center through electron regulation, providing new ideas for the design of high-performance sensing materials [208]. At present, most blood glucose tests rely on blood samples. However, many researchers have proven the potential of using body fluids such as sweat, tears and saliva for detection [209–211]. Zhang et al. have designed a new type of wearable biosensor, which uses Pt SAC to realize high-precision real-time monitoring of glucose in sweat. The sensor adopts a three-dimensional nanostructure, in which the platinum single atom is evenly dispersed on cobalt oxide nanorods and reduced graphene oxide (rGO), showing excellent electrocatalytic performance. Its detection range is wide, up to 1–800 μM, and it has excellent selectivity, stability and anti-interference ability. In addition, this study also designed a flexible sensing device, which adopts a hydrophically modified "S"-shaped micro-flow control channel. Combined with Bluetooth wireless transmission technology, the device can collect sweat glucose signals in real time and display them on smartphones. In the human experiment, the sensor successfully monitored the correlation between sweat glucose and blood glucose fluctuations, providing a new technical way for non-invasive and continuous health monitoring [212]. The design of such wearable biosensors will significantly reduce the pain and inconvenience caused by blood sugar monitoring, thus profoundly changing the lifestyle of patients.

Based on the activity regulation and catalytic mechanism of SACs, different types of sensors can be designed to respond to different detection targets and application scenarios. For example, in the detection of ascorbic acid (AA), Wu et al. reported a iron-cobalt-zinc triple-atom catalyst (FeCoZn-TAC) with oxidase-like activity. This triatomic catalyst can efficiently catalyze oxygen into superoxide anionic free radicals, which reoxidize the color-ding substrate 3,3′,5,5′-tertamethylbenzidine (TMB) to produce blue products. Its synergistic catalytic performance is much better than that of monoatomic or diatomic catalysts. On this basis, the research team has developed a high-sensitivity and high-selectivity ascorbic acid (AA) colorimetric sensing platform with a detection limit as low as 6.24 nM and a linear range of 0.01-90 μM. Its practical application potential in human serum samples has been successfully verified [22]. Qin et al. innovatively anchored platinum single atoms onto $CsPbBr_3$ perovskite nanocrystals (Pt/$CsPbBr_3$ single-atom electrocatalyst) and utilized this composite to modify electrodes. Electrochemical cycling generated a significantly amplified current signal. By measuring this enhanced current, ascorbic acid concentrations could be precisely quantified [213]. Together, these studies demonstrate that precisely engineered single-atom active centers enable the flexible development of high-performance sensors tailored for diverse applications—such as portable screening or precise quantification—offering novel and reliable solutions for disease diagnosis and health monitoring.

Sensors based on SACs can not only detect the above-mentioned glucose and anti-blood acid, but also detect substances such as tumor markers and dopamine. Some SACs even have great potential to realize the integration of diagnosis and treatment. These studies clearly prove the disruptive advantages of SACs. Although there are still

challenges in large-scale precision synthesis and integration with commercial equipment, SAC is undoubtedly pushing medical testing technology towards a future characterized by higher sensitivity, precision, intelligence and accessibility [214–216].

4. Challenges and Outlook

The emergence of SACs marks a revolutionary step in catalytic science in atomic-level precise design and control [217]. Compared with traditional nanozymes, the core advantage of SACs is that their structure is clear and the active site is uniform. This allows researchers to deeply explore its structure-effect relationship and catalytic mechanism, just like studying molecular catalysts, so as to get rid of dependence on complex and heterogeneous nanostructures. They show great potential in the fields of biological sensing, cancer treatment and energy conversion [218]. Although SACs excel in catalytic performance, their clinical applications are still limited by the complexity of biological systems.

Biosafety and long-term toxicity: Metal active sites may be chemically unstable under physiological conditions, resulting in metal ion leakage. This may cause oxidative stress, cell damage, and even organ toxicity. In order to solve this problem, future research should focus on: (1) selecting biocompatible or low-toxic metal elements; (2) improving stability through surface modification (such as polyethylene glycolisation) or bionic packaging to reduce ion release; (3) designing biodegradable carriers to ensure that SACs can be safely removed after using [219,220].

The trade-off between mass production and in vivo stability: The current synthesis method is difficult to maintain the uniformity and structural accuracy of the active site in the process of large-scale preparation, and the cost is high, which limits its practical application. In addition, single atoms are easy to migrate and aggregate in the body, leading to inactivation. The solution includes the development of advanced synthesis methods (such as template method or electrochemical method) and the enhancement of metal-carrier interaction through heteroatomic doping or defect engineering to stabilize single atoms [221].

Poor adaptability to complex biological environments: factors such as pH changes and biomolecular interference will reduce the catalytic activity of SACs or lead to the off-target effect. Inspired by natural enzymes, future SACs should be more intelligent. For example, catalysts can be designed to respond to specific disease signals (such as acidic environments or high concentrations of hydrogen peroxide), or organic frameworks or polymers can be used to simulate enzyme-like microenvironments to improve selectivity and reduce unnecessary interactions [222].

New types of SACs beyond ROS-dependent systems: Current designs often suffer from limited selectivity, potential cytotoxicity, and strong dependence on specific pathological microenvironments, which restricts their broader biomedical applicability. Expanding SACs toward non-ROS catalytic pathways would enable more precise and versatile therapeutic functions. To achieve this, integration with computational chemistry is essential, as data-driven modeling, DFT, and machine learning can guide the rational design of active sites, predict structure–activity relationships, and accelerate the discovery of novel SACs with optimized catalytic performance, stability, and specificity.

Therefore, the future research on SACs needs to be carried out under the framework of multidisciplinary intersection, organically combining safety design, synthesis method optimization, intelligent response function construction and rational design driven by computational chemistry, so as to systematically improve the stability, selectivity and biocompatibility of catalysts. Only in this way can we truly release the transformation potential of SACs in the field of life sciences and promote precision medicine to a new frontier.

Author Contributions

Conceptualization, L.K. and W.W.; Writing—Original Draft Preparation, L.K. and W.L.; Writing—Review & Editing, W.W. and K.Z.; Visualization, L.C. and Y.W.; All the authors discussed the results and commented on the manuscript. All authors have read and agreed to the published version of the manuscript.

Funding

We greatly acknowledge the financial support from National Natural Science Foundation of China (Grant No. 52402353), Sichuan Science and Technology Program (Grant No. 2025ZNSFSC0237).

Institutional Review Board Statement

Not applicable.

Informed Consent Statement

Not applicable.

Data Availability Statement

No new data were generated or analyzed in this study.

Conflicts of Interest

The authors declare no conflict of interest. Given the role as Associate Editors, Kun Zhang had no involvement in the peer review of this paper and had no access to information regarding its peer-review process. Full responsibility for the editorial process of this paper was delegated to another editor of the journal.

Use of AI and AI-Assisted Technologies

During the preparation of this work, the authors used ChatGPT to check and correct sentence structure. After using this tool/service, the authors reviewed and edited the content as needed and take full responsibility for the content of the published article.

References

1. Krajewska, B. Application of Chitin- and Chitosan-Based Materials for Enzyme Immobilizations: A Review. *Enzyme Microb. Technol.* **2004**, *35*, 126–139.
2. Homaei, A.A.; Sariri, R.; Vianello, F.; et al. Enzyme Immobilization: An Update. *J. Chem. Biol.* **2013**, *6*, 185–205.
3. Mohamad, N.R.; Marzuki, N.H.C.; Buang, N.A.; et al. An Overview of Technologies for Immobilization of Enzymes and Surface Analysis Techniques for Immobilized Enzymes. *Biotechnol. Biotechnol. Equip.* **2015**, *29*, 205–220.
4. Breslow, R.; Overman, L.E. "Artificial Enzyme" Combining a Metal Catalytic Group and a Hydrophobic Binding Cavity. *J. Am. Chem. Soc.* **1970**, *92*, 1075–1077.
5. Wilson, M.E.; Whitesides, G.M. Conversion of a Protein to a Homogeneous Asymmetric Hydrogenation Catalyst by Site-Specific Modification with a Diphosphinerhodium(I) Moiety. *J. Am. Chem. Soc.* **1978**, *100*, 306–307.
6. Gao, L.; Zhuang, J.; Nie, L.; et al. Intrinsic Peroxidase-like Activity of Ferromagnetic Nanoparticles. *Nat. Nanotechnol.* **2007**, *2*, 577–583.
7. Manea, F.; Houillon, F.B.; Pasquato, L.; et al. Nanozymes: Gold-Nanoparticle-Based Transphosphorylation Catalysts. *Angew. Chem. Int. Ed.* **2004**, *43*, 6165–6169.
8. Wei, H.; Wang, E. Nanomaterials with Enzyme-like Characteristics (Nanozymes): Next-Generation Artificial Enzymes. *Chem. Soc. Rev.* **2013**, *42*, 6060.
9. Wang, Z.; Li, G.; Gao, Y.; et al. Trienzyme-like Iron Phosphates-Based (FePOs) Nanozyme for Enhanced Anti-Tumor Efficiency with Minimal Side Effects. *Chem. Eng. J.* **2021**, *404*, 125574.
10. Zhong, C.; Hu, C.; Ouyang, D.; et al. Bioinspired Construction of Histidine-Doped Porphyrin Covalent Organic Framework Nanozyme with Enhanced Peroxidase-like Activity for Sensitive Uric Acid Detection. *Chem. Eng. J.* **2023**, *477*, 146979.
11. Liu, D.; Niu, R.; Wang, S.; et al. Correction to "Nitric Oxide-Releasing Mesoporous Hollow Cerium Oxide Nanozyme-Based Hydrogel Synergizes with Neural Stem Cells for Spinal Cord Injury Repair." *ACS Nano* **2025**, *19*, 9432–9432.
12. Luo, L.; Li, J.; Bi, X.; et al. Engineering "Three-in-One" Fluorescent Nanozyme of Ce-Au NCs for on-Site Visual Detection of Hg^{2+}. *J. Hazard. Mater.* **2024**, *476*, 134967.
13. Feng, M.; Li, X.; Zhang, X.; et al. Recent Advances in the Development and Analytical Applications of Oxidase-like Nanozymes. *TrAC Trends Anal. Chem.* **2023**, *166*, 117220.
14. Li, J.; Zhou, Y.; Xiao, Y.; et al. Carbon Dots as Light-Responsive Oxidase-like Nanozyme for Colorimetric Detection of Total Antioxidant Capacity in Fruits. *Food Chem.* **2023**, *405*, 134749.
15. Wang, T.; Liu, T.; Li, Z.; et al. Ultrasmall Gold-Encapsulated Mesoporous Platinum to Promote Photodynamic/Catalytic Therapy through Cascade Enzyme-like Reactions. *J. Colloid Interface Sci.* **2025**, *680*, 117–128.
16. Yu, R.; Xue, J.; Wang, Y.; et al. Novel Ti3C2Tx MXene Nanozyme with Manageable Catalytic Activity and Application to Electrochemical Biosensor. *J. Nanobiotechnol.* **2022**, *20*, 119.

17. Jeon, H.-J.; Kim, H.S.; Chung, E.; et al. Nanozyme-Based Colorimetric Biosensor with a Systemic Quantification Algorithm for Noninvasive Glucose Monitoring. *Theranostics* **2022**, *12*, 6308–6338.
18. Zhou, M.; Feng, J.; Mei, Q.; et al. A Powerful Tumor Catalytic Therapy by an Enzyme-Nanozyme Cascade Catalysis (ENCAT) System. *Small* **2025**, *21*, 2409363.
19. Wan, X.; Ge, Y.; Zhang, J.; et al. A Covalent Organic Framework Derived N-Doped Carbon Nanozyme as the All-Rounder for Targeted Catalytic Therapy and NIR-II Photothermal Therapy of Cancer. *ACS Appl. Mater. Interfaces* **2023**, *15*, 44763–44772.
20. Zhang, W.; Chen, J.; Xie, L. Optical Biosensor Arrays Based on Nanozymes for Environmental Monitoring and Food Safety Detection: Principles, Design, and Applications. *Anal. Methods* **2025**, *17*, 882–891.
21. Cheng, J.; Li, L.; Jin, D.; et al. A Non-metal Single Atom Nanozyme for Cutting off the Energy and Reducing Power of Tumors. *Angew. Chem. Int. Ed.* **2024**, *63*, e202319982.
22. Wu, R.; Sun, M.; Liu, X.; et al. Oxidase-like ZnCoFe Three-Atom Nanozyme as a Colorimetric Platform for Ascorbic Acid Sensing. *Anal. Chem.* **2022**, *94*, 14308–14316.
23. Song, J.; Chen, H.; Lv, Y.; et al. CuO2-Assisting-Zn Single Atom Hybrid Nanozymes for Biofilm-Infected Wound Healing. *Chem. Eng. J.* **2023**, *474*, 145706.
24. Wei, S.; Li, A.; Liu, J.-C.; et al. Direct Observation of Noble Metal Nanoparticles Transforming to Thermally Stable Single Atoms. *Nat. Nanotechnol.* **2018**, *13*, 856–861.
25. Ma, C.; Xu, Y.; Wu, L.; et al. Guided Synthesis of a Mo/Zn Dual Single-Atom Nanozyme with Synergistic Effect and Peroxidase-like Activity. *Angew. Chem. Int. Ed.* **2022**, *61*, e202116170.
26. Qiao, B.; Wang, A.; Yang, X.; et al. Single-Atom Catalysis of CO Oxidation Using Pt1/FeO_x. *Nat. Chem.* **2011**, *3*, 634–641.
27. Huang, L.; Chen, J.; Gan, L.; et al. Single-Atom Nanozymes. *Sci. Adv.* **2019**, *5*, eaav5490.
28. Asakura, K.; Nagahiro, H.; Ichikuni, N.; et al. Structure and Catalytic Combustion Activity of Atomically Dispersed Pt Species at MgO Surface. *Appl. Catal. Gen.* **1999**, *188*, 313–324.
29. Fu, Q.; Saltsburg, H.; Flytzani-Stephanopoulos, M. Active Nonmetallic Au and Pt Species on Ceria-Based Water-Gas Shift Catalysts. *Science* **2003**, *301*, 935–938.
30. Zhang, X.; Shi, H.; Xu, B. Catalysis by Gold: Isolated Surface Au3+ Ions are Active Sites for Selective Hydrogenation of 1,3-Butadiene over Au/ZrO_2 Catalysts. *Angew. Chem.* **2005**, *117*, 7294–7297.
31. Hackett, S.F.J.; Brydson, R.M.; Gass, M.H.; et al. High-Activity, Single-Site Mesoporous Pd/Al2 O3 Catalysts for Selective Aerobic Oxidation of Allylic Alcohols. *Angew. Chem. Int. Ed.* **2007**, *46*, 8593–8596.
32. Liu, P.; Zhao, Y.; Qin, R.; et al. Photochemical Route for Synthesizing Atomically Dispersed Palladium Catalysts. *Science* **2016**, *352*, 797–800.
33. Cao, L.; Liu, W.; Luo, Q.; et al. Atomically Dispersed Iron Hydroxide Anchored on Pt for Preferential Oxidation of CO in H_2. *Nature* **2019**, *565*, 631–635.
34. Tang, J.; Wu, Y.; Li, X.; et al. Single-atom iron catalysts for biomedical applications. *Prog. Mater. Sci.* **2022**, *128*, 100959. https://doi.org/10.1016/j.pmatsci.2022.100959
35. Jiang, Y.; Ran, J.; Mao, K.; et al. Recent Progress in Fenton/Fenton-like Reactions for the Removal of Antibiotics in Aqueous Environments. *Ecotoxicol. Environ. Saf.* **2022**, *236*, 113464.
36. Chen, Y.; Li, Y.; Luo, N.; et al. Kinetic Comparison of Photocatalysis with H2O2-Free Photo-Fenton Process on BiVO4 and the Effective Antibiotic Degradation. *Chem. Eng. J.* **2022**, *429*, 132577.
37. Yan, Q.; Lian, C.; Huang, K.; et al. Constructing an Acidic Microenvironment by MoS2 in Heterogeneous Fenton Reaction for Pollutant Control. *Angew. Chem.-Int. Ed.* **2021**, *60*, 17155–17163.
38. Yang, Y.; Chen, J.; Chen, Z.; et al. Mechanisms of Polystyrene Microplastic Degradation by the Microbially Driven Fenton Reaction. *Water Res.* **2022**, *223*, 118979.
39. Qi, J.; Jiang, G.; Wan, Y.; et al. Nanomaterials-Modulated Fenton Reactions: Strategies, Chemodynamic Therapy and Future Trends. *Chem. Eng. J.* **2023**, *466*, 142960.
40. Lu, Y.; Shi, T.; Liu, W.; et al. Supramonomer-Based Glyco-Cationic Nanoparticles With GSH Depletion-Enhanced Drug/Gene Co-Delivery for Combination Therapy. *Med. Bull.* **2025**, *1*, 171–181.
41. Gong, Y.; Winnik, F.M. Strategies in Biomimetic Surface Engineering of Nanoparticles for Biomedical Applications. *Nanoscale* **2012**, *4*, 360–368.
42. Wang, T.-H.; Shen, M.-Y.; Yeh, N.-T.; et al. Photothermal Nanozymes to Self-Augment Combination Cancer Therapy by Dual-Glutathione Depletion and Hyperthermia/Acidity-Activated Hydroxyl Radical Generation. *J. Colloid Interface Sci.* **2023**, *650*, 1698–1714.
43. Wang, M.; Li, J.; Liu, J.; et al. Smart Nanozymes Coupled with Dynamic Magnet Field and Laser Exposures for Cancer Therapy. *J. Colloid Interface Sci.* **2024**, *676*, 110–126.

44. Zhao, S.; Yang, L.; Wu, J.; et al. Engineering Electron Distribution of Cu2O/FeOx@CNFs p-n Heterojunction Nanozyme: Boosting the Fenton Reaction Efficiency. *J. Mater. Chem. A* **2025**, *13*, 22885–22902.
45. Pei, S.; Wang, S.; Lu, Y.; et al. Application of Metal-Based Catalysts for Fenton Reaction: From Homogeneous to Heterogeneous, from Nanocrystals to Single Atom. *Nano Res.* **2024**, *17*, 9446–9471.
46. Mo, F.; Zhou, Q.; Li, C.; et al. Diatomic Catalysts for Fenton and Fenton-like Reactions: A Promising Platform for Designing/Regulating Reaction Pathways. *Chem. Sci.* **2023**, *14*, 7818–7827.
47. Gao, Y.; Yang, C.; Zhou, M.; et al. Transition Metal and Metal-Nx Codoped MOF-Derived Fenton-Like Catalysts: A Comparative Study on Single Atoms and Nanoparticles. *Small* **2020**, *16*, 2005060.
48. Liang, X.; Wang, D. Activity Regulation of Fenton/Fenton-like Reactions in Single-Atom Catalysis. *Chemcatchem* **2023**, *15*, e202201579.
49. Qiao, W.; Chen, J.; Zhou, H.; et al. A Single-Atom Manganese Nanozyme Mn-N/C Promotes Anti-Tumor Immune Response via Eliciting Type I Interferon Signaling. *Adv. Sci.* **2024**, *11*, 2305979.
50. Chen, Q.; Zhang, M.; Huang, H.; et al. Single Atom-Doped Nanosonosensitizers for Mutually Optimized Sono/Chemo-Nanodynamic Therapy of Triple Negative Breast Cancer. *Adv. Sci.* **2023**, *10*, 2206244.
51. Liu, L.; Zhang, H.; Xing, S.; et al. Copper-Zinc Bimetallic Single-Atom Catalysts with Localized Surface Plasmon Resonance-Enhanced Photothermal Effect and Catalytic Activity for Melanoma Treatment and Wound-Healing. *Adv. Sci.* **2023**, *10*, 2207342.
52. Chen, T.; Han, G.; Li, X. Platinum–Copper Alloy Nanoparticles Armored with Chloride Ion Transporter to Promote Electro-Driven Tumor Inhibition. *Bioact. Mater.* **2022**, *12*, 143–152.
53. Feng, Y.; Qin, J.; Zhou, Y.; et al. Spherical mesoporous Fe-N-C single-atom nanozyme for photothermal and catalytic synergistic antibacterial therapy. *J. Colloid Interface Sci.* **2022**, *606*, 826–836.
54. Chen, B.; Wang, Y.; Mu, M.; et al. Boosting Peroxidase-Mimetic Activity of FeMn-NCe Dual-Atom Radiosensitizing Nanozymes for Augmented Radiodynamic Immunotherapy. *ACS Nano* **2025**, *19*, 10147–10161.
55. Li, C.; Geng, D.; Zhao, W.; et al. Regulation of Gene Expression by FOXA1. *Oncol. Transl. Med.* **2025**, *11*, 282–291.
56. Zhou, X.; Wang, X.; Yang, S.; et al. Advances in Immunotherapy and Targeted Therapy for Pancreatic Cancer. *Oncol. Transl. Med.* **2025**, *11*, 81–91.
57. Zhang, T.; Walsh, A.G.; Yu, J.; et al. Single-Atom Alloy Catalysts: Structural Analysis, Electronic Properties and Catalytic Activities. *Chem. Soc. Rev.* **2021**, *50*, 569–588.
58. Wu, W.; Huang, L.; Wang, E.; et al. Atomic Engineering of Single-Atom Nanozymes for Enzyme-like Catalysis. *Chem. Sci.* **2020**, *11*, 9741–9756.
59. Wang, X.; Wong, K.H.; Yin, Y.; et al. Copper-Doped PDA Nanoparticles with Self-Enhanced ROS Generation for Boosting Photothermal/Chemodynamic Combination Therapy. *Biomater. Sci.* **2025**, *13*, 3903–3914.
60. Feng, G.; Huang, H.; Zhang, M.; et al. Single Atom Iron-Doped Graphic-Phase C3 N4 Semiconductor Nanosheets for Augmented Sonodynamic Melanoma Therapy Synergy with Endowed Chemodynamic Effect. *Adv. Sci.* **2023**, *10*, 2302579.
61. Hua, S.; Dong, X.; Peng, Q.; et al. Single-Atom Nanozymes Shines Diagnostics of Gastrointestinal Diseases. *J. Nanobiotechnology* **2024**, *22*, 286.
62. Guan, J.; Wang, M.; Ma, R.; et al. Single-Atom Rh Nanozyme: An Efficient Catalyst for Highly Sensitive Colorimetric Detection of Acetylcholinesterase Activity and Adrenaline. *Sens. Actuators B Chem.* **2023**, *375*, 132972.
63. Wang, M.; Yang, C.; Chang, M.; et al. Single-Atom Nanozymes Based Nanobee Vehicle for Autophagy Inhibition-Enhanced Synergistic Cancer Therapy. *Nano Today* **2023**, *52*, 101981.
64. Feng, Y.; Shi, Y.; Zhao, Q.; et al. Onion-like Carbon Based Single-Atom Iron Nanozyme for Photothermal and Catalytic Synergistic Antibacterial Application. *J. Colloid Interface Sci.* **2025**, *681*, 205–214.
65. Yang, M.-D.; Zhu, C.-Y.; Yang, G.; et al. Camouflaged Membrane-Bridged Radionuclide/Mn Single-Atom Enzymes Target Lipid Metabolism Disruption to Evoke Antitumor Immunity. *Mil. Med. Res.* **2025**, *12*, 59.
66. Sun, M.; Liu, X.; Liu, Z.; et al. Single-Atom Catalysts Mediated Bioorthogonal Modulation of N6 -Methyladenosine Methylation for Boosting Cancer Immunotherapy. *J. Am. Chem. Soc.* **2024**, *146*, 8216–8227.
67. Tian, Q.; Huangfu, S.; Kang, G.; et al. High-Spin States of Manganese(III) Enable Robust Cold-Adapted Activity of MnO2 Nanozymes. *Adv. Sci.* **2025**, *12*, 2415477.
68. Han, B.; Li, T.; Zhang, J.; et al. A Highly Active Rh1 /CeO2 Single-Atom Catalyst for Low-Temperature CO Oxidation. *Chem. Commun.* **2020**, *56*, 4870–4873.
69. Huang, F.; Peng, M.; Chen, Y.; et al. Low-Temperature Acetylene Semi-Hydrogenation over the Pd1 –Cu1 Dual-Atom Catalyst. *J. Am. Chem. Soc.* **2022**, *144*, 18485–18493.
70. Qin, T.; Chen, Y.; Miao, X.; et al. Low-Temperature Adaptive Single-Atom Iron Nanozymes against Viruses in the Cold Chain. *Adv. Mater.* **2024**, *36*, 2309669.

71. Joshi, R.M.; Telang, B.; Soni, G.; et al. Overview of Perspectives on Cancer, Newer Therapies, and Future Directions. *Oncol. Transl. Med.* **2024**, *10*, 105–109.
72. Pu, Y.; Duan, Y.; Li, W.; et al. A Cerium Single-Atom Catalyst Enables Targeted Catalytic Therapy for Acute Kidney Injury via Neutrophil Hitchhiking. *J. Controlled Release* **2025**, *380*, 404–416.
73. Xu, S.; Yuan, Y.; Pan, Y.; et al. A Highly Efficient and Biocompatible Cupper-Based Single-Atom Nanocatalyst with Unsaturated Coordination Structure for Efficient Diabetic Wound Healing. *Small* **2025**, *21*, 2502896.
74. Jin, X.; Guo, F.; Wu, M.; et al. Emerging Versatile Nanozymes for the Therapeutic and Diagnostic Applications of Diseases. *J. Transl. Med.* **2025**, *23*, 1375.
75. Jiang, Y.; Rong, H.; Wang, Y.; et al. Single-Atom Cobalt Nanozymes Promote Spinal Cord Injury Recovery by Anti-Oxidation and Neuroprotection. *Nano Res.* **2023**, *16*, 9752–9759.
76. Qiao, G.; Li, S.; Liu, J.; et al. Engineered Probiotics Secreting IL-18BP and Armed with Dual Single-Atom Catalysts for Synergistic Therapy in Ulcerative Colitis. *ACS Appl. Mater. Interfaces* **2025**, *17*, acsami.5c11356.
77. Sun, L.; Li, W.; Liu, Z.; et al. Iodine-Doped Single-Atom Cobalt Catalysts with Boosted Antioxidant Enzyme-like Activity for Colitis Therapy. *Chem. Eng. J.* **2023**, *453*, 139870.
78. Dai, S.; Yao, L.; Liu, L.; et al. Carbon Dots-Supported Zn Single Atom Nanozymes for the Catalytic Therapy of Diabetic Wounds. *Acta Biomater.* **2024**, *186*, 454–469.
79. Li, B.; Bai, Y.; Yion, C.; et al. Single-Atom Nanocatalytic Therapy for Suppression of Neuroinflammation by Inducing Autophagy of Abnormal Mitochondria. *ACS Nano* **2023**, *17*, 7511–7529.
80. Liu, M.; Xu, W.; Tang, Y.; et al. Tuning Atomically Dispersed Metal Sites in Nanozymes for Sensing Applications. *Angew. Chem. Int. Ed.* **2025**, *64*, e202424070.
81. Chen, J.; Lian, T.; Liu, S.; et al. Iron-Carbon Dots Embedded in Molybdenum Single-Atom Nanoflowers as Multifunctional Nanozyme for Dual-Mode Detection of Hydrogen Peroxide and Uric Acid. *J. Colloid Interface Sci.* **2024**, *667*, 450–459.
82. Gao, X.; Wei, H.; Ma, W.; et al. Inflammation-Free Electrochemical in Vivo Sensing of Dopamine with Atomic-Level Engineered Antioxidative Single-Atom Catalyst. *Nat. Commun.* **2024**, *15*, 7915.
83. He, H.; Wang, H.H.; Liu, J.; et al. Research Progress and Application of Single-Atom Catalysts: A Review. *Molecules* **2021**, *26*, 6501.
84. Cai, D.; Zhang, J.; Kong, Z.; et al. Synergistic Effect of Single-Atom Catalysts and Vacancies of Support for Versatile Catalytic Applications. *ChemCatChem* **2024**, *16*, e202301414.
85. Xue, H.; Li, Y.; Ma, X.; et al. Enhancing the Antioxidant Capacity of Fe Single-Atom Nanozymes through Local Coordination Manipulation for Psoriasis Treatment. *Mater. Today Bio* **2025**, *32*, 101830.
86. Zhang, S.; Ruan, W.; Guan, J. Single-Atom Nanozymes for Antibacterial Applications. *Food Chem.* **2024**, *456*, 140094.
87. Liao, G.; Zhang, L.; Li, C.; et al. Emerging Carbon-Supported Single-Atom Catalysts for Biomedical Applications. *Matter* **2022**, *5*, 3341–3374.
88. Ye, H.; Lai, Y.; Wu, Z.; et al. Carbon-Based Nanozymes: Catalytic Mechanisms, Performance Tuning, and Environmental and Biomedical Applications. *Anal. Methods* **2025**, *17*, 6264–6281.
89. Batool, I.; Anwar, A.; Imran, M.; et al. Prospecting Carbon-Based Nanomaterials for Harnessing Multienzyme-Like Activities. *Top. Catal.* **2025**, *68*, 823–855.
90. Yu, B.; Sun, W.; Lin, J.; et al. Using Cu-Based Metal–Organic Framework as a Comprehensive and Powerful Antioxidant Nanozyme for Efficient Osteoarthritis Treatment. *Adv. Sci.* **2024**, *11*, 2307798.
91. Liu, Y.; Zhao, H.; Zhao, Y. Designing Efficient Single Metal Atom Biocatalysts at the Atomic Structure Level. *Angew. Chem. Int. Ed.* **2024**, *63*, e202315933.
92. Bi, R.; Liu, J.; Cai, Y.; et al. Dual-Atom Nanozymes: Synthesis, Characterization, Catalytic Mechanism and Biomedical Applications. Colloids Surf. *B Biointerfaces* **2025**, *253*, 114774.
93. Shen, J.; Chen, J.; Qian, Y.; et al. Atomic Engineering of Single-Atom Nanozymes for Biomedical Applications. *Adv. Mater.* **2024**, *36*, 2313406.
94. Wang, Z.; Wang, W.; Wang, J.; et al. Single-Atom Catalysts with Ultrahigh Catalase-Like Activity Through Electron Filling and Orbital Energy Regulation. *Adv. Funct. Mater.* **2023**, *33*, 2209560.
95. Fei, H.; Dong, J.; Feng, Y.; et al. General Synthesis and Definitive Structural Identification of MN4C4 Single-Atom Catalysts with Tunable Electrocatalytic Activities. *Nat. Catal.* **2018**, *1*, 63–72.
96. Liu, J.; Xiao, J.; Luo, B.; et al. Central Metal and Ligand Effects on Oxygen Electrocatalysis over 3d Transition Metal Single-Atom Catalysts: A Theoretical Investigation. *Chem. Eng. J.* **2022**, *427*, 132038.
97. Hou, X.; Ding, J.; Liu, W.; et al. Asymmetric Coordination Environment Engineering of Atomic Catalysts for CO2 Reduction. *Nanomaterials* **2023**, *13*, 309.
98. Song, P.; Wang, Y.; Pan, J.; et al. Structure-Activity Relationship in High-Performance Iron-Based Electrocatalysts for Oxygen Reduction Reaction. *J. Power Sources* **2015**, *300*, 279–284.

99. Shen, H.; Gracia-Espino, E.; Ma, J.; et al. Atomically FeN2 Moieties Dispersed on Mesoporous Carbon: A New Atomic Catalyst for Efficient Oxygen Reduction Catalysis. *Nano Energy* **2017**, *35*, 9–16.
100. Liang, X.; Wang, D.; Zhao, Z.; et al. Coordination Number Dependent Catalytic Activity of Single-Atom Cobalt Catalysts for Fenton-Like Reaction. *Adv. Funct. Mater.* **2022**, *32*, 2203001.
101. Liu, Y.; Wang, B.; Zhu, J.; et al. Single-Atom Nanozyme with Asymmetric Electron Distribution for Tumor Catalytic Therapy by Disrupting Tumor Redox and Energy Metabolism Homeostasis. *Adv. Mater.* **2023**, *35*, 2208512.
102. Chen, Y.; Jiang, B.; Hao, H.; et al. Atomic-Level Regulation of Cobalt Single-Atom Nanozymes: Engineering High-Efficiency Catalase Mimics. *Angew. Chem. Int. Ed.* **2023**, *62*, e202301879.
103. Mao, S.; Liu, C.; Wu, Y.; et al. Porous P, Fe-Doped g-C3N4 Nanostructure with Enhanced Photo-Fenton Activity for Removal of Tetracycline Hydrochloride: Mechanism Insight, DFT Calculation and Degradation Pathways. *Chemosphere* **2022**, *291*, 133039.
104. Fan, M.; Cui, J.; Wu, J.; et al. Improving the Catalytic Activity of Carbon-Supported Single Atom Catalysts by Polynary Metal or Heteroatom Doping. *Small* **2020**, *16*, 1906782.
105. Ye, B.; Li, W.; Zhang, X.; et al. Advancing Heterogeneous Organic Synthesis with Coordination Chemistry-Empowered Single-Atom Catalysts. *Adv. Mater.* **2024**, *36*, 2402747.
106. Wu, F.; Liu, P. Surface Organometallic Chemistry for Single-Site Catalysis and Single-Atom Catalysis. *Chem. Res. Chin. Univ.* **2022**, *38*, 1139–1145.
107. Long, Y.; Xiao, G.; Dai, J.; et al. Efficacy and Durability of Cobalt Sulfide Nanoparticles and Axial Sulfur-Coordinated Cobalt Single-Atom Composite Sites in Hydrogenative Nitroaromatics Decontamination. *J. Colloid Interface Sci.* **2025**, *684*, 540–551.
108. Lu, W.; Chen, S.; Li, C.; et al. A Bifunctional S-Doped Fe-N-C Nanozyme with Excellent Oxidase-like Activity and Photothermal Effect for Tumor Diagnosis and Treatment. *Mater. Today Commun.* **2023**, *37*, 107049.
109. Gao, P.; Liang, G.; Ru, T.; et al. Phosphorus Coordinated Rh Single-Atom Sites on Nanodiamond as Highly Regioselective Catalyst for Hydroformylation of Olefins. *Nat. Commun.* **2021**, *12*, 4698.
110. Sun, J.; Li, K.; Liu, Z.; et al. Construction of Electron-Rich Nickel Single Atom Catalyst by Heteroatom Doping for Enhanced CO_2 Electroreduction. *J. Catal.* **2025**, *445*, 116020.
111. Tao, X.; Liu, Y.; Lu, R.; et al. Phosphorus-Enhanced Bimetallic Single-Atom Catalysts for Hydrogen Evolution. *Adv. Energy Mater.* **2025**, *15*, 2404167.
112. Li, K.; Zhang, S.; Zhang, X.; et al. Atomic Tuning of Single-Atom Fe–N–C Catalysts with Phosphorus for Robust Electrochemical CO_2 Reduction. *Nano Lett.* **2022**, *22*, 1557–1565.
113. Zhang, J.; Sun, B.; Shi, S.; et al. Heteroatom-Doped Cobalt Single-Atomic Nanozymes with Differential Enzyme-like Activity for Bacteria-Infected Wound Therapy. *J. Colloid Interface Sci.* **2024**, *675*, 580–591.
114. He, J.; Zhao, Z.-H.; Li, J.; et al. Hydrogenation of Olefinic Bonds in Nitrile Butadiene Rubber on Single-Atom Pd1/CeO2−x Catalysts with Ultrahigh Mass Activity and Stability. *Chem. Eng. J.* **2024**, *487*, 150427.
115. Zhang, Z.; Han, X.; Zhang, J.; et al. Revolutionizing Photothermal CO2 Hydrogenation with Ceria-Based Catalysts. *Nano Res.* **2025**, *18*, 94906998.
116. Li, R.; Luo, L.; Ma, X.; et al. Single Atoms Supported on Metal Oxides for Energy Catalysis. *J. Mater. Chem. A* **2022**, *10*, 5717–5742.
117. Zhang, L.; Bi, H.; Wang, Z.; et al. Insight into Enhanced Hydrogen Evolution of Single-Atom Cu1/TiO_2 Catalysts from First Principles. *Int. J. Hydrog. Energy* **2022**, *47*, 4653–4661.
118. Pei, W.; Yang, K.; Deng, J.; et al. SO_2-Tolerant Mesoporous Iron Oxide Supported Bimetallic Single Atom Catalyst for Methanol Removal. *Appl. Catal. B Environ.* **2023**, *335*, 122888.
119. Tu, L.; Liu, R.; Zhao, D.; et al. PtPd/TiO_2 Catalysts for Low-Temperature Toluene Oxidation. *Catal. Surv. Asia* **2021**, *25*, 389–398.
120. Hu, B.; Sun, K.; Zhuang, Z.; et al. Distinct Crystal-Facet-Dependent Behaviors for Single-Atom Palladium-On-Ceria Catalysts: Enhanced Stabilization and Catalytic Properties. *Adv. Mater.* **2022**, *34*, 2107721.
121. Fu, N.; Liang, X.; Wang, X.; et al. Controllable Conversion of Platinum Nanoparticles to Single Atoms in Pt/CeO2 by Laser Ablation for Efficient CO Oxidation. *J. Am. Chem. Soc.* **2023**, *145*, 9540–9547.
122. Pham, H.N.; DeLaRiva, A.; Peterson, E.J.; et al. Designing Ceria/Alumina for Efficient Trapping of Platinum Single Atoms. *ACS Sustain. Chem. Eng.* **2022**, *10*, 7603–7612.
123. Zhu, T.; Han, Y.; Liu, S.; et al. Porous Materials Confining Single Atoms for Catalysis. *Front. Chem.* **2021**, *9*, 717201.
124. Xue, K.; Mo, Y.; Long, B.; et al. Single-atom Catalysts Supported on Ordered Porous Materials: Synthetic Strategies and Applications. *InfoMat* **2022**, *4*, e12296.
125. Haroon, H.; Xiang, Q. Single-Atom Based Metal–Organic Framework Photocatalysts for Solar-Fuel Generation. *Small* **2024**, *20*, 2401389.

126. Liu, Y.; Zhang, X.; Wang, Z.; et al. Zeolite-Anchored Single-Atom Catalysts for Enhanced Hydrogenation and Dehydrogenation Reaction Process. *Adv. Mater.* 2025, e13175.
127. Alonso, G.; López, E.; Huarte-Larrañaga, F.; et al. Zeolite-Encapsulated Single-Atom Catalysts for Efficient CO2 Conversion. J. CO_2 Util. **2021**, *54*, 101777.
128. Chen, Q.; Peng, P.; Yang, G.; et al. Template-Guided Regioselective Encaging of Platinum Single Atoms into Y Zeolite: Enhanced Selectivity in Semihydrogenation and Resistance to Poisoning. *Angew. Chem. Int. Ed.* **2022**, *61*, e202205978.
129. Xiao, J.; Zhang, T.; Wang, Q. Metal–Organic Framework Derived Single-Atom Catalysts for CO_2 Conversion to Methanol. *Curr. Opin. Green Sustain. Chem.* **2022**, *37*, 100660.
130. Ma, S.; Han, W.; Han, W.; et al. Recent Advances and Future Perspectives in MOF-Derived Single-Atom Catalysts and Their Application: A Review. *J. Mater. Chem. A* **2023**, *11*, 3315–3363.
131. Qu, W.; Chen, C.; Tang, Z.; et al. Progress in Metal-Organic-Framework-Based Single-Atom Catalysts for Environmental Remediation. *Coord. Chem. Rev.* **2023**, *474*, 214855.
132. Yu, S.; Kang, H.; Jee, S.; et al. MOF-Based Single-Atom and Metal Cluster Catalysts by Room-Temperature Synthesis for Tumor Therapy. *Adv. Healthc. Mater.* **2025**, *14*, 2501058.
133. Xue, W.; Song, X.; Mei, D. Theoretical Insights into CO Oxidation over MOF-808-Encapsulated Single-Atom Metal Catalysts. *J. Phys. Chem. C* **2021**, *125*, 17097–17108.
134. Wang, L.; Dou, Y.; Gan, R.; et al. The Single Atom Anchoring Strategy: Rational Design of MXene-Based Single-Atom Catalysts for Electrocatalysis. *Small* **2025**, *21*, 2410772.
135. Yang, C.; Zhao, Z.; Liu, Q. Mechanistic Insight into the Dispersion Behavior of Single Platinum Atom on Monolayer G-C3N4 in Single-Atom Catalysts from Density Functional Theory Calculations. *Appl. Surf. Sci.* **2021**, *566*, 150697.
136. Lv, L.; Shen, Y.; Liu, J.; et al. Computational Screening of High Activity and Selectivity TM/g-C3 N4 Single-Atom Catalysts for Electrocatalytic Reduction of Nitrates to Ammonia. *J. Phys. Chem. Lett.* **2021**, *12*, 11143–11150.
137. Xu, M.; Yu, Y.; Shi, G.; et al. Curved Surface of Graphitic Carbon Nitride Boosting Cyclohexane Oxidation over Single-Atom Catalysts. *ACS Appl. Nano Mater.* **2024**, *7*, 11952–11964.
138. Bai, X.; Guan, J. Applications of MXene-Based Single-Atom Catalysts. *Small Struct.* **2023**, *4*, 2200354.
139. Park, D.; Hong, S.; Han, J.; et al. Insights into the Synergy Effect in Dual Single-Atom Catalysts on Defective CeO2 under CO2 Hydrogenation. *Appl. Catal. B Environ. Energy* **2025**, *365*, 124987.
140. Zhao, Y.; Lu, B.; An, Z.; et al. Insight into the Mechanism on NO Reduction over Dual-Atom Fe-Cu Catalyst Supported on N-Dopped Graphene: A DFT Study. *Appl. Surf. Sci.* **2025**, *682*, 161769.
141. Chen, Z.; Su, X.; Ding, J.; et al. Boosting Oxygen Reduction Reaction with Fe and Se Dual-Atom Sites Supported by Nitrogen-Doped Porous Carbon. *Appl. Catal. B Environ.* **2022**, *308*, 121206.
142. Liu, D.; Srinivas, K.; Chen, X.; et al. Dual Fe, Zn Single Atoms Anchored on Carbon Nanotubes Inlaid N, S-Doped Hollow Carbon Polyhedrons for Boosting Oxygen Reduction Reaction. *J. Colloid Interface Sci.* **2022**, *624*, 680–690.
143. Gao, Y.; Liu, B.; Wang, D. Microenvironment Engineering of Single/Dual-Atom Catalysts for Electrocatalytic Application. *Adv. Mater.* **2023**, *35*, 2209654.
144. Ma, Q.; Liu, Y.; Zhu, H.; et al. Nanozymes in Tumor Theranostics. *Front. Oncol.* **2021**, *11*, 666017.
145. Yu, Q. Immune Resistance to ICIs in pMMR/MSS mCRC Due to a Suppressive TIME. *Oncol. Transl. Med.* **2025**.
146. Lu, X.; Gao, S.; Lin, H.; et al. Single-Atom Catalysts for Nanocatalytic Tumor Therapy. *Small* **2021**, *17*, 2004467.
147. He, W.; Wu, J.; Liu, J.; et al. Single-Atom Nanozymes for Catalytic Therapy: Recent Advances and Challenges. *Adv. Funct. Mater.* **2024**, *34*, 2312116.
148. Phan, N.M.; Nguyen, T.L.; Kim, J. Nanozyme-Based Enhanced Cancer Immunotherapy. *Tissue Eng. Regen. Med.* **2022**, *19*, 237–252.
149. Wang, X.; Wei, N.; Zhang, Y.; et al. Nanozyme-Mediated Glutathione Depletion for Enhanced ROS-Based Cancer Therapies: A Comprehensive Review. *Nanomed.* **2025**, *20*, 279–290.
150. Zhu, X.; Xu, N.; Zhang, L.; et al. Novel Design of Multifunctional Nanozymes Based on Tumor Microenvironment for Diagnosis and Therapy. *Eur. J. Med. Chem.* **2022**, *238*, 114456.
151. Wang, S.; Hu, Z.; Wei, Q.; et al. Precise Design of Atomically Dispersed Fe, Pt Dinuclear Catalysts and Their Synergistic Application for Tumor Catalytic Therapy. *ACS Appl. Mater. Interfaces* **2022**, *14*, 20669–20681.
152. Wang, W.; Zhu, Y.; Zhu, X.; et al. Biocompatible Ruthenium Single-Atom Catalyst for Cascade Enzyme-Mimicking Therapy. *ACS Appl. Mater. Interfaces* **2021**, *13*, 45269–45278.
153. Li, Z.; Ding, B.; Li, J.; et al. Multi-Enzyme Mimetic MoCu Dual-Atom Nanozyme Triggering Oxidative Stress Cascade Amplification for High-Efficiency Synergistic Cancer Therapy. *Angew. Chem. Int. Ed.* **2025**, *64*, e202413661.
154. Wang, Y.; Chen, K.; Ou, Y.; et al. A TME-Responsive Nanocatalytic Platform for Synergistically Enhanced Chemodynamic Therapy through Calcium Overload for Precision Cancer Treatment. *Carbon* **2025**, *245*, 120833.
155. Zhao, M.; Yang, R.; Wei, Y.; et al. Dual Isolated Bimetal Single-Atom Catalysts for Tumor ROS Cycle and Parallel Catalytic Therapy. *Nano Today* **2022**, *44*, 101493.

156. Geng, B.; Hu, J.; He, X.; et al. Single Atom Catalysts Remodel Tumor Microenvironment for Augmented Sonodynamic Immunotherapy. *Adv. Mater.* **2024**, *36*, 2313670.
157. Zhu, Y.; Gong, P.; Wang, J.; et al. Amplification of Lipid Peroxidation by Regulating Cell Membrane Unsaturation To Enhance Chemodynamic Therapy. *Angew. Chem. Int. Ed.* **2023**, *62*, e202218407.
158. Liu, Y.; Yao, M.; Han, W.; et al. Construction of a Single-Atom Nanozyme for Enhanced Chemodynamic Therapy and Chemotherapy. *Chem. Eur. J.* **2021**, *27*, 13418–13425.
159. Cheng, J.; Li, L.; Jin, D.; et al. Boosting Ferroptosis Therapy with Iridium Single-Atom Nanocatalyst in Ultralow Metal Content. *Adv. Mater.* **2023**, *35*, 2210037.
160. Shao, B.; Zhu, Y.; Du, Y.; et al. Mn-Doped Single Atom Nanozyme Composited Au for Enhancing Enzymatic and Photothermal Therapy. *J. Colloid Interface Sci.* **2022**, *628*, 419–434.
161. Fang, X.; Yang, D.; Wu, X.; et al. Theoretical Calculation-Guided Engineering of Fe-Mn Based Dual-Center Single-Atom Catalysts for Synergistic Tumor Therapy. *Chem. Eng. J.* **2023**, *474*, 145675.
162. Pei, J.; Dou, H.; Liu, C.; et al. Manganese Single-Atom Nanostructures for Highly Efficient Tumor Therapy. *J. Ind. Eng. Chem.* **2022**, *109*, 330–337.
163. Xing, Y.; Xiu, J.; Zhou, M.; et al. Copper Single-Atom Jellyfish-like Nanomotors for Enhanced Tumor Penetration and Nanocatalytic Therapy. *ACS Nano* **2023**, *17*, 6789–6799.
164. Sharma, S.K.; Shrivastava, N.; Rossi, F.; et al. Nanoparticles-Based Magnetic and Photo Induced Hyperthermia for Cancer Treatment. *Nano Today* **2019**, *29*, 100795.
165. Wang, L.; Qu, X.; Zhao, Y.; et al. Exploiting Single Atom Iron Centers in a Porphyrin-like MOF for Efficient Cancer Phototherapy. *ACS Appl. Mater. Interfaces* **2019**, *11*, 35228–35237.
166. Chang, M.; Hou, Z.; Wang, M.; et al. Single-Atom Pd Nanozyme for Ferroptosis-Boosted Mild-Temperature Photothermal Therapy. *Angew. Chem. Int. Ed.* **2021**, *60*, 12971–12979.
167. Qi, P.; Zhang, J.; Bao, Z.; et al. A Platelet-Mimicking Single-Atom Nanozyme for Mitochondrial Damage-Mediated Mild-Temperature Photothermal Therapy. *ACS Appl. Mater. Interfaces* **2022**, *14*, 19081–19090.
168. Zhang, M.; Song, X.; Qin, Y.; et al. Single-Atom–Doped Piezocatalyst Induces Copper-Free Cuproptosis in Tumor Therapy. *Sci. Adv.* **2025**, *11*, eadt8451.
169. Tsvetkov, P.; Coy, S.; Petrova, B.; et al. Copper Induces Cell Death by Targeting Lipoylated TCA Cycle Proteins. *Science* **2022**, *375*, 1254–1261.
170. Dixon, S.J.; Lemberg, K.M.; Lamprecht, M.R.; et al. Ferroptosis: An Iron-Dependent Form of Nonapoptotic Cell Death. *Cell* **2012**, *149*, 1060–1072.
171. Ma, J.; Dang, X.; Xue, Y.; et al. Vanadium Single-Atom Nanozyme Boosts Cuproptosis/Ferroptosis/Apoptosis Combined with Photothermal-Enhanced Tumor Therapy through Dual Catalytic Activity. *ACS Appl. Bio Mater.* **2025**, *8*, 10195–10205.
172. Xu, R.; Chen, J.; Dong, L.; et al. Ferroptosis Therapy of Colorectal Cancer by Single Co Atom Supported on Fe-Based Zeolitic Imidazolate Frameworks. *ACS Appl. Nano Mater.* **2024**, *7*, 20438–20444.
173. Liu, Y.; Li, G.; Zhang, T.; et al. Driving Multifunctional Nanomedicine Design for Non-Inflammatory Tumor Therapy with Integrated Machine Learning and Density Functional Theory. *Adv. Mater.* **2025**, *37*, 2503576.
174. Wang, J.; Wu, J.; Ma, Z.; et al. Nature-Inspired Cell Membrane-Coated Artificial Biocatalysts with Os-Single-Atom Sites and Multienzyme-Mimetic Activities for Targeted Tumor Therapy. *Chem. Eng. J.* **2025**, *520*, 166190.
175. Wen, D.; Feng, J.; Deng, R.; et al. Zn/Pt Dual-Site Single-Atom Driven Difunctional Superimposition-Augmented Sonosensitizer for Sonodynamic Therapy Boosted Ferroptosis of Cancer. *Nat. Commun.* **2024**, *15*, 9359.
176. Zhou, J.; Xu, D.; Tian, G.; et al. Coordination-Driven Self-Assembly Strategy-Activated Cu Single-Atom Nanozymes for Catalytic Tumor-Specific Therapy. *J. Am. Chem. Soc.* **2023**, *145*, 4279–4293.
177. Ye, J.; Lv, W.; Li, C.; et al. Tumor Response and NIR-II Photonic Thermal Co-Enhanced Catalytic Therapy Based on Single-Atom Manganese Nanozyme. *Adv. Funct. Mater.* **2022**, *32*, 2206157.
178. Yin, Y.; Ge, X.; Ouyang, J.; et al. Tumor-Activated in Situ Synthesis of Single-Atom Catalysts for O2-Independent Photodynamic Therapy Based on Water-Splitting. *Nat. Commun.* **2024**, *15*, 2954.
179. Deng, H.; Li, X.; Pan, L.; et al. Single-Atom W Anchored Hexagonal Boron Nitride Piezoelectric Nanosonosensitizer Remodels Tumor Microenvironment for Enhanced Sonodynamic Therapy. *Adv. Funct. Mater.* **2025**, *35*, 2420974.
180. Sies, H. Role of Metabolic H_2O_2 Generation. *J. Biol. Chem.* **2014**, *289*, 8735–8741.
181. Singh, S. Antioxidant Nanozymes as Next-Generation Therapeutics to Free Radical-Mediated Inflammatory Diseases: A Comprehensive Review. *Int. J. Biol. Macromol.* **2024**, *260*, 129374.
182. Zhang, H.; Zhou, G.; Li, C.; et al. Activation of the cGAS/STING Pathway Contributes to Neuroinflammation in Diabetes-Associated Cognitive Decline. *Med. Bull.* **2025**, *1*, 200–212.
183. Chen, Q.; Zhang, X. Research Advances on Nanozyme-Guided Therapy of Inflammatory Bowel Diseases★. *Acta Chim. Sin.* **2023**, *81*, 1043.

184. Wang, Y.; Mu, M.; Fan, R.; et al. Single-Atom Enzymes: From Nano-Enzyme Evolution to the Biomedical Frontier of Precision Catalysis. *Coord. Chem. Rev.* **2026**, *549*, 217317.
185. Tagaras, N.; Song, H.; Sahar, S.; et al. Safety Landscape of Therapeutic Nanozymes and Future Research Directions. *Adv. Sci.* **2024**, *11*, 2407816.
186. Wang, H.; Chen, X.; Mao, M.; et al. Multifaceted Therapy of Nanocatalysts in Neurological Diseases. *J. Biomed. Nanotechnol.* **2021**, *17*, 711–743.
187. Pu, Y.; Huang, S.; Gao, S.; et al. Cerium Single-Atom Catalysts-Armed Lactobacillus Reuteri for Multipronged Anti-Inflammatory/Anti-Fibrotic Therapy of Inflammatory Bowel Disease. Acta Pharm. *Sin. B* **2025**, *15*, 5400–5415.
188. Chu, D.; Zhao, M.; Rong, S.; et al. Dual-Atom Nanozyme Eye Drops Attenuate Inflammation and Break the Vicious Cycle in Dry Eye Disease. *Nano-Micro Lett.* **2024**, *16*, 120.
189. Kuai, L.; Huang, F.; Mao, L.; et al. Single-Atom Catalysts with Isolated Cu1 -N4 Sites for Atopic Dermatitis Cascade Catalytic Therapy via Activating PPAR Signaling. *Small* **2024**, *20*, 2407365.
190. Huang, B.; Tang, T.; Chen, S.-H.; et al. Near-Infrared-IIb Emitting Single-Atom Catalyst for Imaging-Guided Therapy of Blood-Brain Barrier Breakdown after Traumatic Brain Injury. *Nat. Commun.* **2023**, *14*, 197.
191. Xiang, J.; Yang, X.; Tan, M.; et al. NIR-Enhanced Pt Single Atom/g-C3N4 Nanozymes as SOD/CAT Mimics to Rescue ATP Energy Crisis by Regulating Oxidative Phosphorylation Pathway for Delaying Osteoarthritis Progression. *Bioact. Mater.* **2024**, *36*, 1–13.
192. Zhou, X.; Guo, Z.; Li, Y.-B.; et al. Cobalt Single-Atom Catalysts on MnO_2 for Regulating Reactive Oxygen Species toward Robust Elimination of Antibiotic-Resistance Threats from Water. *Sep. Purif. Technol.* **2026**, *388*, 136794.
193. Shi, T.; Cui, Y.; Yuan, H.; et al. Burgeoning Single-Atom Nanozymes for Efficient Bacterial Elimination. *Nanomaterials* **2023**, *13*, 2760.
194. Zhao, Y.; Yu, Y.; Gao, F.; et al. A Highly Accessible Copper Single-Atom Catalyst for Wound Antibacterial Application. *Nano Res.* **2021**, *14*, 4808–4813.
195. Yang, L.; Yang, H.; Yin, S.; et al. Fe Single-Atom Catalyst for Efficient and Rapid Fenton-Like Degradation of Organics and Disinfection against Bacteria. *Small* **2022**, *18*, 2104941.
196. Zigale, T.T.; Huang, R.; Wang, L.; et al. Co–N4 -Coordinated Single-Atom Nanozymes with Dual Bactericidal-Regenerative Functions: Overcoming Tetracycline Resistance through Self-Enhanced Oxidase-Mimicking Catalysis. *ACS Appl. Mater. Interfaces* **2026**, *18*, 3669–3683.
197. Zhang, Z.; Yang, T.; Wang, J.; et al. Hollow Mesoporous Molybdenum Single-Atom Nanozyme-Based Reactor for Enhanced Cascade Catalytic Antibacterial Therapy. *Int. J. Nanomedicine* **2023**, *18*, 7209–7223.
198. Li, Z.; Xu, D.; Deng, Z.; et al. Single-Atom-Catalyzed MXene-Based Nanoplatform with Photo-Enhanced Peroxidase-Like Activity Nanotherapeutics for Staphylococcus Aureus Infection. *Chem. Eng. J.* **2023**, *452*, 139587.
199. Zhang, M.; Xu, W.; Gao, Y.; et al. Manganese–Iron Dual Single-Atom Catalyst with Enhanced Nanozyme Activity for Wound and Pustule Disinfection. *ACS Appl. Mater. Interfaces* **2023**, *15*, 42227–42240.
200. Fan, X.; Gao, Y.; Yang, F.; et al. A Copper Single-Atom Cascade Bionanocatalyst for Treating Multidrug-Resistant Bacterial Diabetic Ulcer. *Adv. Funct. Mater.* **2023**, *33*, 2301986.
201. Ge, H.; Wang, M.; Wei, X.; et al. Copper-Based Nanozymes: Potential Therapies for Infectious Wounds. *Small* **2025**, *21*, 2407195.
202. Dai, S.; Jiang, L.; Liu, L.; et al. MOF-Encapsulated Copper-Doped Carbon Dots Nanozymes with Excellent Biological Activity Promote Diabetes Wound Healing. *Regen. Biomater.* **2024**, *11*, rbae119.
203. Wang, J.; Li, Y.; Huang, D.; et al. Rapid Inactivation of Droplet-Transmitted Microorganisms Using Silver-Single-Atom Photocatalysts Impregnated Masks under Weak Solar Irradiation. *Chem. Eng. J.* **2024**, *483*, 149309.
204. Jin, X.; Gao, F.; Qin, M.; et al. How to Make Personal Protective Equipment Spontaneously and Continuously Antimicrobial (Incorporating Oxidase-like Catalysts). *ACS Nano* **2022**, *16*, 7755–7771.
205. Li, Z.; Tian, E.; Wang, S.; et al. Single-Atom Catalysts: Promotors of Highly Sensitive and Selective Sensors. *Chem. Soc. Rev.* **2023**, *52*, 5088–5134.
206. Wang, Z.; Wu, J.; Wei, W.; et al. Pt Single-Atom Electrocatalysts at Cu_2O Nanowires for Boosting Electrochemical Sensing toward Glucose. *Chem. Eng. J.* **2024**, *495*, 153564.
207. Yan, M.; Xiong, C.; Han, X.; et al. Single-Atom Catalysts Enabled Electrochemical Sensing for Glucose. *Biosens. Bioelectron.* **2025**, *273*, 117144.
208. Qi, C.; Kong, Y.; Qi, X.; et al. Adjacent Se Site Boosts Electrocatalytic Activity of Ni Single Atoms for Realizing Highly Sensitive Electrochemical Glucose Sensing. *Chem. Eng. J.* **2025**, *522*, 167703.
209. Dai, X.-Y.; Shi, X.-J.; Wu, Y.; et al. A Self-Assembled Gold-Spiked Nanosphere Based Paper Assay for Sensitive Glucose Detection. *Anal. Methods* **2025**, *17*, 4002–4008.
210. Pathmanathan, P.; Gomathi, A.; Ramesh, A.; et al. In Situ Generation of Turbostratic Nickel Hydroxide as a Nanozyme for Salivary Glucose Sensor. *RSC Adv.* **2024**, *14*, 21808–21820.

211. Cui, Y.; Zhang, H.; Zhu, J.; et al. Correlations of Salivary and Blood Glucose Levels among Six Saliva Collection Methods. *Int. J. Environ. Res. Public. Health* **2022**, *19*, 4122.
212. Zhang, Y.; Yang, Z.; Qiao, C.; et al. Synergistic Enhancement of Wearable Biosensor through Pt Single-Atom Catalyst for Sweat Analysis. *Biosens. Bioelectron.* **2024**, *258*, 116354.
213. Qin, Y.; Chen, H.; Luo, Y.; et al. Platinum Single Atom on CsPbBr3 Nanocrystals as Electrocatalyst Boosts Electrochemical Sensing of Ascorbic Acid. *Talanta* **2024**, *277*, 126396.
214. Wei, W. Single-Atom Nanozymes towards Central Nervous System Diseases. *Nano Res.* **2023**, *16*, 5121–5139.
215. Chellasamy, G.; Arumugasamy, S.K.; Nam, M.J.; et al. Experimental and Simulation Studies of Bioinspired Au-Enhanced Copper Single Atom Catalysts towards Real-Time Expeditious Dopamine Sensing on Human Neuronal Cell. *Chem. Eng. J.* **2023**, *471*, 144842.
216. Yang, Y.; Wei, X.; Chen, S.; et al. Recent Advances in Single-Atom Materials Prompted Photoelectrochemical Sensing. *Electroanalysis* **2025**, *37*, e70000.
217. Wang, A.; Li, J.; Zhang, T. Heterogeneous Single-Atom Catalysis. *Nat. Rev. Chem.* **2018**, *2*, 65–81.
218. Cheng, N.; Zhang, L.; Doyle-Davis, K.; et al. Single-Atom Catalysts: From Design to Application. *Electrochem. Energy Rev.* **2019**, *2*, 539–573.
219. Wang, L.; Yang, Q.; Huo, M.; et al. Engineering Single-Atomic Iron-Catalyst-Integrated 3D-Printed Bioscaffolds for Osteosarcoma Destruction with Antibacterial and Bone Defect Regeneration Bioactivity. *Adv. Mater.* **2021**, *33*, 2100150.
220. Cai, S.; Liu, J.; Ding, J.; et al. Tumor-Microenvironment-Responsive Cascade Reactions by a Cobalt-Single-Atom Nanozyme for Synergistic Nanocatalytic Chemotherapy. *Angew. Chem. Int. Ed.* **2022**, *61*, e202204502.
221. Li, J.; Zhang, L.; An, X.; et al. Tuning Adsorbate-Mediated Strong Metal-Support Interaction by Oxygen Vacancy: A Case Study in Ru/TiO_2. *Angew. Chem.* **2024**, *136*, e202407025.
222. Wang, Y.; Gao, F.; Li, X.; et al. Tumor Microenvironment-Responsive Fenton Nanocatalysts for Intensified Anticancer Treatment. *J. Nanobiotechnol.* **2022**, *20*, 69.